

# Introspective analysis of convolutional neural networks for improving discrimination performance and feature visualisation

Shakeel Shafiq<sup>1</sup>, Tayyaba Azim<sup>Corresp. 1</sup>

<sup>1</sup> Center of Excellence in IT, Institute of Management Sciences (IMSciences), Peshawar, Peshawar, KPK, Pakistan

Corresponding Author: Tayyaba Azim

Email address: tayyaba.azim@imsciences.edu.pk

Deep neural networks have been widely explored and utilised as a useful tool for feature extraction in computer vision and machine learning. It is often observed that the last fully connected (FC) layers of convolutional neural network possess higher discrimination power as compared to the convolutional and maxpooling layers whose goal is to preserve local and low-level information of the input image and down sample it to avoid overfitting. Inspired from the functionality of local binary pattern (LBP) operator, this paper proposes to induce discrimination into the mid layers of convolutional neural network by introducing a discriminatively boosted alternative to pooling (DBAP) layer that has shown to serve as a favourable replacement of early maxpooling layer in a convolutional neural network (CNN). A thorough research of the related works show that the proposed change in the neural architecture is novel and has not been proposed before to bring enhanced discrimination and feature visualisation power achieved from the mid layer features. The empirical results reveal that the introduction of DBAP layer in popular neural architectures such as AlexNet and LeNet produces competitive classification results in comparison to their baseline models as well as other ultra-deep models on several benchmark data sets. In addition, better visualisation of intermediate features can allow one to seek understanding and interpretation of black box behaviour of convolutional neural networks, used widely by the research community.

# 1 Introspective Analysis of Convolutional Neural 2 Networks for Improving Discrimination 3 Performance and Feature Visualisation

4 Shakeel Shafiq<sup>1</sup> and Tayyaba Azim<sup>1</sup>

5 <sup>1</sup>Center of Excellence in IT, Institute of Management Sciences, Peshawar, Pakistan.

6 Corresponding author:

7 Tayyaba Azim<sup>1</sup>

8 Email address: tayyaba.azim@imsciences.edu.pk

## 9 ABSTRACT

10 Deep neural networks have been widely explored and utilised as a useful tool for feature extraction in computer  
11 vision and machine learning. It is often observed that the last fully connected (FC) layers of convolutional neural  
12 network possess higher discrimination power as compared to the convolutional and maxpooling layers whose goal  
13 is to preserve local and low-level information of the input image and down sample it to avoid overfitting. Inspired  
14 from the functionality of local binary pattern (LBP) operator, this paper proposes to induce discrimination into the mid  
15 layers of convolutional neural network by introducing a discriminatively boosted alternative to pooling (DBAP) layer  
16 that has shown to serve as a favourable replacement of early maxpooling layer in a convolutional neural network  
17 (CNN). A thorough research of the related works show that the proposed change in the neural architecture is novel  
18 and has not been proposed before to bring enhanced discrimination and feature visualisation power achieved from  
19 the mid layer features. The empirical results reveal that the introduction of DBAP layer in popular neural architectures  
20 such as AlexNet and LeNet produces competitive classification results in comparison to their baseline models as well  
21 as other ultra-deep models on several benchmark data sets. In addition, better visualisation of intermediate features  
22 can allow one to seek understanding and interpretation of black box behaviour of convolutional neural networks,  
23 used widely by the research community.

## 24 1 INTRODUCTION

25 Deep learning architectures such as convolutional neural networks, recurrent neural networks and deep  
26 belief networks have been applied to a wide range of applications in domains such as natural language pro-  
27 cessing, speech recognition, computer vision, and bioinformatics, where they have produced outstanding  
28 results approximately the same and in some scenarios better than the humans (He et al., 2015; Silver et al.,  
29 2016; LeCun et al., 1990; Szegedy et al., 2015; Girshick et al., 2014; Hinton et al., 2012; Yu et al., 2018;  
30 Zhang et al., 2016; Masumoto et al., 2019; Le and Nguyen, 2019; Le, 2019; Do et al., 2020). Among these  
31 deep models, convolutional neural network (CNN) is the most popular choice for automatically learning  
32 visually discriminative features memorised by the fully connected layers. The interest of researchers in  
33 CNN triggered when Krizhevsky et al. (Krizhevsky et al., 2012) showed record beating performance  
34 on ImageNet 2012 object classification data set with their CNN (AlexNet), achieving an error rate of  
35 16.4% in comparison to 26.1% error shown by the runner up. Ever since then, various variants of deep  
36 convolutional models such as Visual Geometry Group (VGG)-VD (Very Deep) model (Simonyan and  
37 Zisserman, 2014), GoogLeNet/Inception (Szegedy et al., 2015) and ResNet (He et al., 2016) have been  
38 introduced, increasing the depth of the models from 8 layers in AlexNet to 152 layers in ResNet. These  
39 models have not just progressed in depth but also their intricacy of connectivity, type of activation function  
40 and the training algorithm that prevents the diminishing gradient issue observed during training through  
41 back propagation in ultra deep models.

42 Keeping in account the success of deep neural models, many researchers have treated CNN as a black  
43 box feature extractor where end-to-end learning framework is utilised to draw discriminative features  
44 from the last fully connected (FC) layers. The last fully connected layers are successfully utilised to  
45 extract global image descriptors as they possess rich high level semantic information that can effectively

distinguish the object of interest from the background (Sharif Razavian et al., 2014). In contrast, the intermediate layers of CNN are popular for extracting spatial and local characteristics of images which are important to extract expressive regions of objects, yet cannot serve very well as a global image descriptor. To get improved performance on different classification tasks, most of the researchers have focused on increasing the *depth* of the convolutional neural model and varied the network's training strategy and activation functions (Bengio et al., 2013a; LeCun et al., 2015). We observe that designing and training such an *ultra-deep* architecture for global feature extraction is: (i) Expensive in terms of computation, (ii) results in model size large in terms of disk space utilisation and memory usage, (iii) prone to overfitting when the data set size is limited, and (iv) requires a large amount of labelled training data when fine tuning the model for new application domains. On account of these challenges, we take an introspective approach to understand the functionality and behaviour of the intermediate layers, in particular the convolutional and pooling layers of CNN, and propose a novel technique to improve their *representational power* along with increasing the *discrimination performance* of the model without going deeper with additional hidden layers. Visualisation of features allows one to functionally understand and interpret the behaviour of deep model's internal layers in connection to its progressive depth and output (Raghu et al., 2017; Poole et al., 2016). Visualising the representational capacity of deep models has been a topic of recent interest to express general priors about the world that can help one identify the stimuli causing a certain output and ultimately design learning machines that can solve different AI tasks (Bengio et al., 2013b; Zeiler and Fergus, 2013; Mordvintsev et al., 2015; Raghu et al., 2017; Santos and Abel, 2019). The topic has grabbed interest of the research community so much so that dedicated workshops in leading conferences like NIPS and CVPR are arranged to discuss the works under this theme. We have therefore laid our focus on developing a technique that can transform features from model's intermediate layers into a visually powerful tool for introspective analysis, as well as act as discriminative off the shelf feature extractor for image classification with simple and sophisticated machine learning classifiers. Our empirical results reveal that with the proposed technique, intermediate layers close to the input layer could also be made more competent for feature visualisation and discrimination tasks.

The main contributions of this work are outlined as follows: (1) Improving the classification performance of classical CNN architectures: LeNet and AlexNet on benchmark data sets without increasing their depth (hidden layers), (2) Improving the visualisation power of features learned by the intermediate layers of CNN, (3) Introducing discriminatively boosted alternative to pooling (DBAP) layer in the CNN architectures, that can serve independently as an efficient feature extractor for classification when used with classifiers such as  $k$ -nearest neighbour ( $k$ -NN) and support vector machines (SVM). The pretrained CNN with DBAP layer offers features that could be deployed in resource constrained environments where ultra-deep models could not be stored, retrieved and trained.

The remaining paper is structured as follows: Section 2 discusses the related research work carried out in the area of computer vision. Section 3 provides preliminary information required to understand the details of proposed methodology discussed in Section 4. Section 5 discusses the benchmark data sets, implementation details and evaluates the results of conducted experiments. We conclude this work in Section 6 with a discussion on the future work intended to further improve and extend this research in future. There is also a supplementary section (Section 7) that holds additional results to provide in depth analysis of the proposed change in convolutional neural models.

## 2 RELATED WORK

There has been a recent surge of interest in understanding and visualising the intermediate layers of deep models for interpretability and explainability, leading to the development of more stable and reliable machine learning systems (Zeiler and Fergus, 2014; Ren et al., 2019; Bau et al., 2019; Hazard et al., 2019; Gagne et al., 2019; Hohman et al., 2018). The visualisation techniques allow the researchers and practitioners understand what features are being learned by the deep model at each stage. Visualisation diagnostics may also serve as an important debugging tool to improve a model's performance, make comparisons and select optimal model parameters for the task at hand. This often requires monitoring the model during the training phase, identifying misclassified examples and then testing the model on a handful of well-known data instances to observe performance. Generally, the following parameters of deep model are visualised either during or after the training phase: (1) Weights on the neural connections (Smilkov et al., 2017), (2) convolutional filters (Zeiler and Fergus, 2014; Yosinski et al., 2015) (3) neuron activations in response to a single or group of instances (Goodfellow et al., 2016; Yosinski et al., 2015),

100 (4) gradients for the measurement and distribution of train error (D. Cashman and Chang, 2017), and  
101 (5) model metrics such as loss and accuracy computed at each epoch. This work focuses on improving  
102 the visualisation power of deep neural models in addition to enhancing their discrimination ability as a  
103 classifier and feature extractor.

104 The fully connected (FC) layers of deep convolutional neural network have often been utilised to  
105 extract features due to their higher discriminative ability and semantic representation of image concepts  
106 that makes them a powerful global descriptor (Simonyan and Zisserman, 2014; He et al., 2016). The  
107 FC features have demonstrated their advantage over VLAD (Vector of Locally Aggregated Descriptors)  
108 and Fisher vector descriptors and are known to be invariant to illumination and rotation to some extent,  
109 however they lack the description of local patterns captured by the convolutional layers. To address  
110 this limitation, some researchers have proposed to utilise the intermediate layers of deep models to  
111 improve their performance on various tasks (Cimpoi et al., 2015; Babenko and Lempitsky, 2015; Liu  
112 et al., 2017b; Yue-Hei Ng et al., 2015; Liu et al., 2015). For instance, Ng et al. (Ng et al., 2015)  
113 aggregated convolutional layer activations using vector of locally aggregated descriptors (VLAD) and  
114 achieved competitive performance on image retrieval task. Tolias et al. (Tolias et al., 2015) max pooled  
115 the activations of the last convolutional layer to represent each image patch and achieved compelling  
116 performance for object retrieval. Lie et al. (Liu et al., 2017a) built a powerful image representation using  
117 activations from two consecutive convolutional layers to recognise images. Kumar et al. (Kumar et al.,  
118 2009, 2012) introduced the use of Volterra theory for the first time to learn discriminative convolution  
119 filters (DCF) from the pixel features on gray-level images.

120 In addition to the convolutional layers, researchers have also explored the use of various types of  
121 pooling functions from simple ones such as max, average, and stochastic pooling to complex ones, like  
122 spatial pyramid pooling network (SPP-Net), which allows the convolutional neural model to take images  
123 of variable scales using spatial pyramid aggregation scheme (He et al., 2014). The pooling layers have  
124 traditionally been utilised in CNN to avoid overfitting by reducing the size of the detected features by a  
125 factor of two. However, the fact that they lose spatial information and keep no track of the relationship  
126 between the features extracted by the convolutional layers, makes them less appealing and strongly  
127 criticised by front end researchers like Geoffrey Hinton. In order to avoid the limitations of pooling  
128 operations, it is suggested to use dynamic routing (routing-by-agreement) scheme, in replacement of the  
129 max-pooling operation and name this newly proposed model as Capsule Network (Sabour et al., 2017).  
130 Springenberg et al. (Springenberg et al., 2014) also proposed to discard the pooling layer in favour  
131 of architecture that only consists of repeated convolutional layers. In order to reduce the size of the  
132 representation, he suggested using larger stride in convolutional layer once in a while. Discarding pooling  
133 layers has also been found important in training good generative models, such as variational autoencoders  
134 (VAEs) or generative adversarial networks (GANs) (Yu et al., 2017). From these moves, it seems likely  
135 that the future architectures will feature very few to no pooling layers.

136 Keeping in view these recent trends of research to improve deep models as classifiers, we hereby  
137 take inspiration from the characteristics of local binary pattern (LBP) operator, known widely for its  
138 simplicity and discriminative power to improve the representational power of CNN's intermediate layers  
139 and utilise it for gaining better discrimination performance on image classification task. Similar work has  
140 been carried out by Xu et al. (Juefei et al., 2017), who proposed an efficient non-linear approximation  
141 of convolutional layers in the convolutional neural network. Their proposed model namely local binary  
142 convolutional neural networks (LBCNN) (Juefei et al., 2017) utilises a hybrid combination of fixed sparse  
143 and learnable weights and local binary patterns (LBP). In contrast, this work deploys dense weights and  
144 resides on regularisation techniques like dropout and batch normalisation to avoid overfitting issues.

### 145 **3 PRELIMINARIES**

#### 146 **3.1 Local Binary Patterns**

147 Local binary pattern (LBP) is a non-parametric approach that extracts local features of images by compar-  
148 ing the intensity of each center pixel in a patch with adjacent pixels in its defined neighbourhood (Ojala  
149 et al., 1994). If the neighbours have intensity greater than the center pixel, they are assigned the value of  
150 1, otherwise 0. LBP has traditionally worked well with window patches of size  $3 \times 3$ ,  $5 \times 5$  and  $7 \times 7$ , etc,  
151 scanned through the image in an overlapping fashion. This bit string is read sequentially in a specified  
152 order and is mapped to a decimal number (using base 2) as the feature value assigned to the central pixel.  
153 These aggregate feature values represent the local texture in the image. The parameters and configurations

154 of LBP could be tweaked by customising the window size, base, pivot (pixel treated as physical center of  
155 the patch) and ordering (clockwise/ anticlockwise encoding).

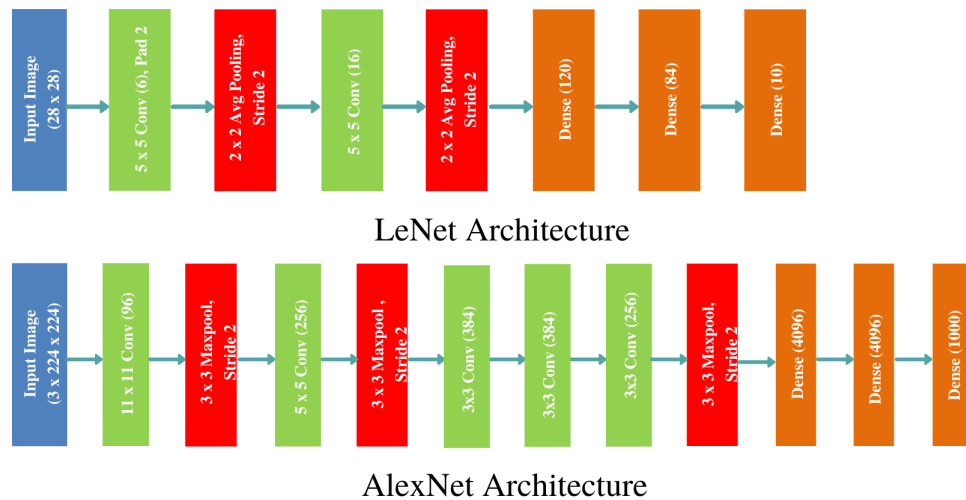


**Figure 1.** Classical CNN architectures: LeNet (LeCun et al., 1998) and AlexNet (Krizhevsky et al., 2012) used to outperform the state of the art image classification results on MNIST and ImageNet data sets.

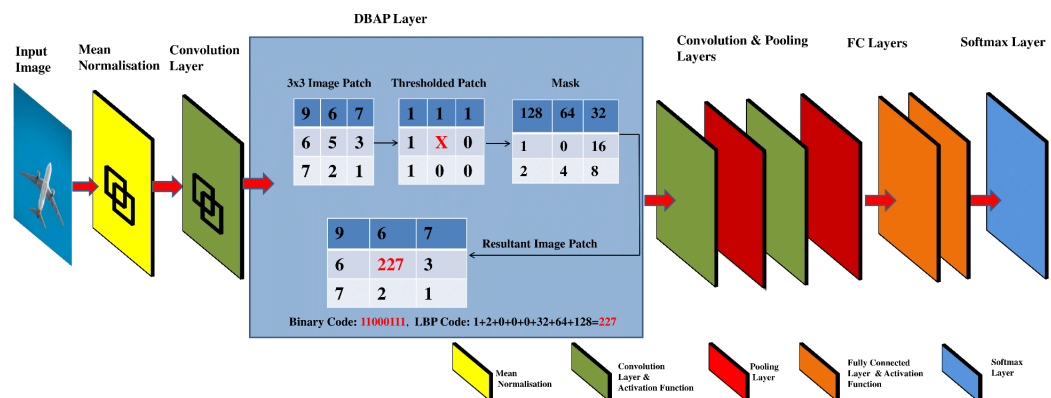


**Figure 2.** Graphical abstract of DBAP layer embedded in classical convolutional neural network models for boosting discrimination performance and feature visualisation power.

### 156 3.2 Convolutional Neural Networks (CNN)

157 Convolutional neural network (CNN) is a multi-layered feed forward artificial neural network consisting  
158 of neurons in different layers to detect high level features from visual patterns automatically. Unlike  
159 the traditional feature extraction approaches where the features are hand engineered, CNN draws the  
160 features automatically by retaining their temporal and spatial information. The classical architecture of  
161 CNN consists of the following layers: (a) Input layer, (b) Convolutional layer, (c) Pooling layer, (d) Fully  
162 Connected/Dense layer and (e) Output layer. Except for the input and output layers, the remaining layers  
163 change their order and count giving rise to various types of neural architectures.

164 Ever since the successful exhibit of CNN for large scale image classification and retrieval (Krizhevsky  
165 et al., 2012), various architectures of CNN have been proposed that alter the hidden layers' order, count,  
166 types of activation functions and learning algorithm to improve the model's discrimination performance  
167 and retrieval speed. We have chosen two popular architectures: LeNet and AlexNet to showcase the

168 efficacy of the proposed approach on benchmark data sets. LeNet is the pioneering neural network  
 169 proposed by Yann LeCun consisting of 7 layers (5 hidden), and is known to work very well for recognising  
 170 digits and zip codes (LeCun et al., 1998). AlexNet, named after Alex Krizhevsky (Krizhevsky et al.,  
 171 2012), is a groundbreaking CNN consisting of five convolutional and three fully connected layers showing  
 172 outstanding performance on large scale image recognition data set. The two architectures are demonstrated  
 173 in Figure 1. The gradient of CNN's cost function is computed through backpropagation algorithm and the  
 174 model parameters are updated through stochastic gradient descent (SGD) learning algorithm.

## 175 4 METHODOLOGY

---

### Algorithm 1 Discriminatively Boosted Alternative to Pooling (DBAP) Layer in CNN.

---

**Input:** Input Image,  $X^{(j)} = \{x_i^{(j)}\}_{i=1}^d$ ; Filter Size,  $F$ ; Stride,  $S$ ; Number of Neighbours,  $P$ ; Index of Neighbour,  $p$ ;  
 Kernel,  $K$ .

**Output:** DBAP features,  $1 \times d$

```

1: while not converge do
2:   for Each Image do
3:     Mean normalise the incoming image pixels  $X^{(j)}$  and store them in  $X_{norm}^{(j)}$ .
4:     Compute the convolutional features from normalised image  $X_{norm}^{(j)}$  by convolving kernel  $K$ .
5:     Apply activation function on convolved features to map them in non-linear space.
6:     Forward propagate the non-linear result of activation function to DBAP layer.
7:     Partition the received image into overlapping blocks of equal size using the stride,  $S$  and filter size,  $F$ .
8:     Compute the LBP for each block using formula:
9:      $LBP_{R,P} = \sum_{p=0}^{P-1} s(g_p - g_c) \cdot 2^p$ ,
       where  $s(g_p - g_c) = 1$  if  $g_p \geq g_c$ , 0 otherwise.
       % Here  $g_p$  and  $g_c$  denote the gray values of the central pixel and its neighbours.
10:    Concatenate all the feature blocks represented by DBAP layer and forward pass the learned features in
       vectorised form to the next layer in CNN.
11:    Continue forward pass and perform backpropagation to learn model parameters.
12:   end for
13: end while

```

---

176 In order to enhance the discrimination power and representation capability of intermediate layers in  
 177 CNN, we reformulate its architecture by introducing a discriminatively boosted alternative to pooling  
 178 (DBAP) layer embedded at early stage of feature learning. Figure 1 demonstrates how LeNet and AlexNet  
 179 models stack convolutional and pooling layers to learn local spatial features. We first preprocess each  
 180 input image by performing *standardization* approach. The goal of standardization is to bring all the  
 181 features at the same scale so that each feature is treated equally important and none dominates the other  
 182 during features learning. Each image pixel  $x_i^{(j)}$  is standardized by computing the mean,  $\mu_i$  and standard  
 183 deviation,  $\sigma_i$  of each feature  $i$  in an image  $j$  by utilising the following formula:

$$x_i^{(j)} = \frac{x_i^{(j)} - \mu_i}{\sigma_i} \quad (1)$$

184 Standardizing input data is a common approach used in neural networks and machine learning in  
 185 general, to learn parameters, optimise and converge the models faster (Xiang and Li, 2017). After doing  
 186 standardization, the  $d$  dimensional features are passed to the convolutional layer to capture the local  
 187 features of the image. This result is next passed to the activation function to map the learned features  
 188 in a non-linear space. Conventionally, the CNN architecture forward propagates the result of activation  
 189 functions to a pooling layer that uses  $2 \times 2$  filter window to down sample the features detected in non-linear  
 190 space. The proposed framework replaces the first pooling layer of CNN with an alternative layer named  
 191 as discriminatively boosted alternative to pooling (DBAP) layer. See Figure 2 for illustration of the  
 192 proposed changes in the CNN architecture. The DBAP layer takes its inspiration from local binary pattern  
 193 (LBP) operator that acts as a powerful descriptor to summarise the characteristics of local structures  
 194 in an image. The layer processes the features received from the previous layer by following the steps

195 outlined in Algorithm 1. A  $3 \times 3$  window with replicated boundary pixel padding is deployed to capture  
 196 the local features of the image. Each pixel in the image is treated as a pivot (center pixel) to replace  
 197 its intensity in connection to the intensity of pixels in its surrounding defined by the filter window. For  
 198 each image patch, the neighbouring pixel values acquire the value 1 if their magnitude is equivalent or  
 199 greater than the magnitude of the centre pixel. The magnitude is taken as 0 otherwise. For the example  
 200 demonstrated in Figure 2, the resulting LBP value for the center pixel is 11000111, equivalent to 227 in  
 201 decimal number system. We move the filter one stride forward to compute LBP feature for each pixel in  
 202 the image. For the given filter size, the DBAP layer computes 8-bit binary values for all the image pixels  
 203 and converts them into their decimal equivalent. These values are totally based on the properties of the  
 204 pixels in relationship to their neighbours. Our proposed DBAP layer is non-parametric and extracts more  
 205 discriminative and visually powerful features as compared to the maxpooling layer used in benchmark  
 206 CNN architectures. After processing the data through DBAP layer, it is forward propagated to the next  
 207 layers in each architecture (LeNet and AlexNet) and treated in a conventional manner. In LeNet, this  
 208 information passes on to the following layers in sequence: Convolutional, Pooling, Fully Connected, Fully  
 209 Connected, and Fully Connected layers, whereas in AlexNet, the flow of information after DBAP takes  
 210 the following route in sequence: Convolutional, Pooling, Convolutional, Convolutional, Convolutional,  
 211 Pooling, Fully Connected, Fully Connected, Fully Connected layers. We discuss the implementation  
 212 details regarding CNN model's training and testing in Section 5.

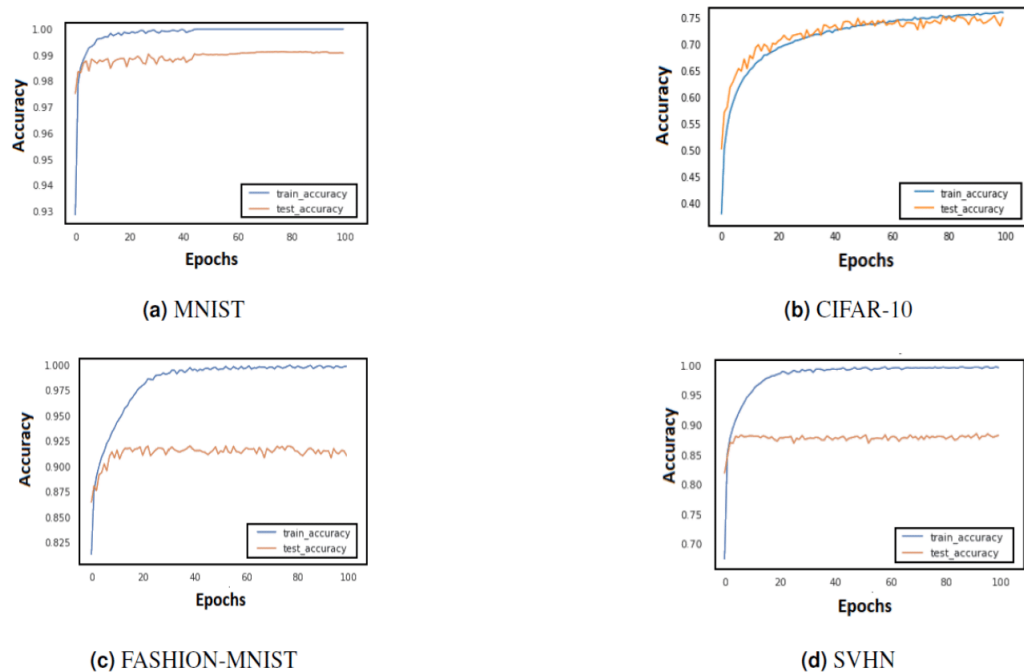


**Figure 3.** Train and test accuracy curves of LeNet with DBAP layer are demonstrated on state-of-the-art benchmark data sets. The softmax activation function is used to enable LeNet for classification task.

## 213 5 EXPERIMENTS AND RESULTS

### 214 5.1 Data Sets Used

215 We have evaluated the efficacy of the proposed approach on different benchmark data sets with baseline  
 216 convolutional neural networks and their other very deep counterparts such as GoogleNet (Szegedy et al.,  
 217 2015), LBCNN (Juefei et al., 2017) and MobileNet (Howard et al., 2017). There are four standard data sets  
 218 used in this paper: MNIST, SVHN, FASHION-MNIST and CIFAR-10. These are benchmark computer  
 219 vision data sets that are well understood and highly used by the researchers to provide basis for any  
 220 improvement in the proposed learning algorithm or neural architecture. Their popularity has won them a

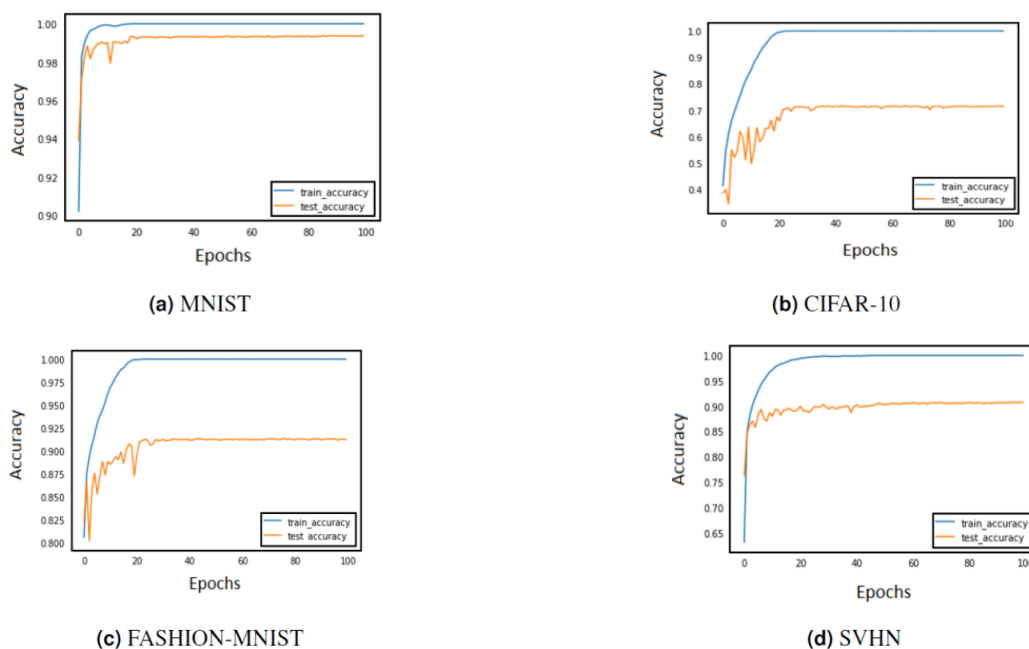


**Figure 4.** Train and test accuracy curves of AlexNet with DBAP layer are demonstrated on state-of-the-art benchmark data sets. The softmax activation function is used to enable AlexNet for classification task.

regular place in many deep learning frameworks such as Keras, TensorFlow and Torch. Consequently, their off the shelf use is constantly on the rise, more than PASCAL VOC and ImageNet data sets till date <sup>1</sup>

The Modified National Institute of Standards and Technology (MNIST) data set (LeCun et al., 1989) consists of 60,000 training and 10,000 test images of hand written digits with a resolution of  $28 \times 28$  pixels. The database contains grayscale images of digits 0 to 9. Despite the success of deep models with large scale data sets, MNIST enjoys the title of most widely used test bed in deep learning, surpassing CIFAR 10 (Krizhevsky and Hinton, 2009) and ImageNet (Deng et al., 2009) in its popularity via Google trends<sup>2</sup>. We have therefore selected this data set to benchmark the results of our proposed approach with state of the art comparative methods.

The FASHION-MNIST (F-MNIST) data set (Xiao et al., 2017) comprises of  $28 \times 28$  grayscale images of 70,000 fashion products belonging to 10 different categories: TShirt/Top, Trouser, Pullover, Dress, Coat, Sandals, Shirt, Sneaker, Bag, Ankle boot. Similar to MNIST, the training set of FASHION-MNIST also comprises of 60,000 train images and 10,000 test set images.

The Street View House Numbers (SVHN) (Netzer et al., 2011) is a real world image data set consisting of digits in natural scenes of street houses. The digits 0 to 9 offer a multi-class classification problem with spatial resolution of  $32 \times 32$  pixels. The data distribution consists of 73,257 train digits and 26,032 test digits for performance evaluation. These images show vast intra-class variations and include complex photometric distortions making the recognition problem a challenge just as in a general-purpose object recognition or natural scene understanding system.

The CIFAR-10 data set (Krizhevsky et al., 2014) contains 60,000 color images from 10 different classes: Trucks, cats, cars, horses, airplanes, ships, dogs, birds, deer and frogs. The images have spatial dimension of  $32 \times 32$  pixels. The data set consists of 5 training batches with each batch comprising of 10,000 train images. The test batch contains 10,000 images with 1000 randomly-selected images from each class.

<sup>1</sup><https://trends.google.com/trends/explore?date=all&q=mnist,%2F11hz37p042,ImageNet>

<sup>2</sup><https://trends.google.com/trends/explore?date=all&q=mnist,CIFAR,ImageNet>

### 245 5.2 Tools Used and Computational Requirements of the Proposed Model

246 The proposed neural model with DBAP layer was trained on Google Colab's (col, 2019) Tesla K-  
 247 80 graphics processing unit (GPU) using Keras (Chollet et al., 2015) and TensorFlow deep learning  
 248 frameworks implemented in Python. Colab is a cloud based service that allows researchers to develop deep  
 249 learning applications with free GPU support. The system used had Intel(R) Xeon(R) 2.3GHz processor  
 250 with two cores and 16GB of RAM. To achieve results in optimal time, it is recommended to run the deep  
 251 learning framework on premium GPU cards with at least 8GB of RAM.

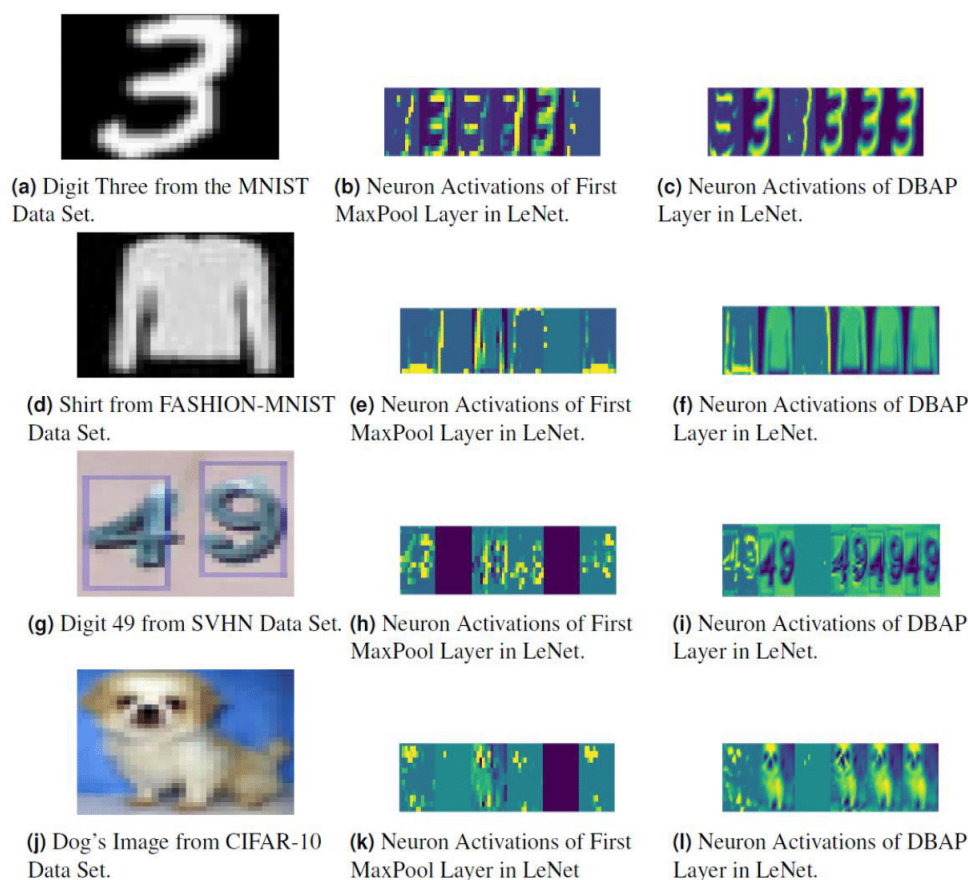


**Figure 5.** Visualising the response of neurons in the MaxPool layer and DBAP layer present in baseline LeNet and LeNet with DBAP layer respectively. With 6 filters/kernels deployed in the first MaxPool layer of LeNet, one can observe that the visualisations of DBAP layer demonstrate more meaningful information about the input image as compared to the MaxPool layer.

### 252 5.3 Evaluation Metrics Used for Monitoring Classification Performance

253 The evaluation metrics used to monitor the quality of classification framework are accuracy, precision,  
 254 recall, F1-score, and, area under the curve (AUC). These are standard model evaluation metrics used  
 255 in research to carry out investigation and perform analysis (Le, 2019; Do et al., 2020). Accuracy is not  
 256 regarded as a good measure of judging model's performance when the class distribution is imbalanced,  
 257 i.e. when the number of samples between two or more classes vary significantly. Such imbalance can  
 258 affect the traditional classifiers as well as the deep models, commonly resulting in poor performances  
 259 over the minority classes. Since, class instances of all the data sets used in this work are not balanced (in  
 260 specific SVHN), we have demonstrated precision, recall, F-1 score, and receiver operating characteristics  
 261 (in addition to accuracy to judge the performance of the proposed features and classifiers.)

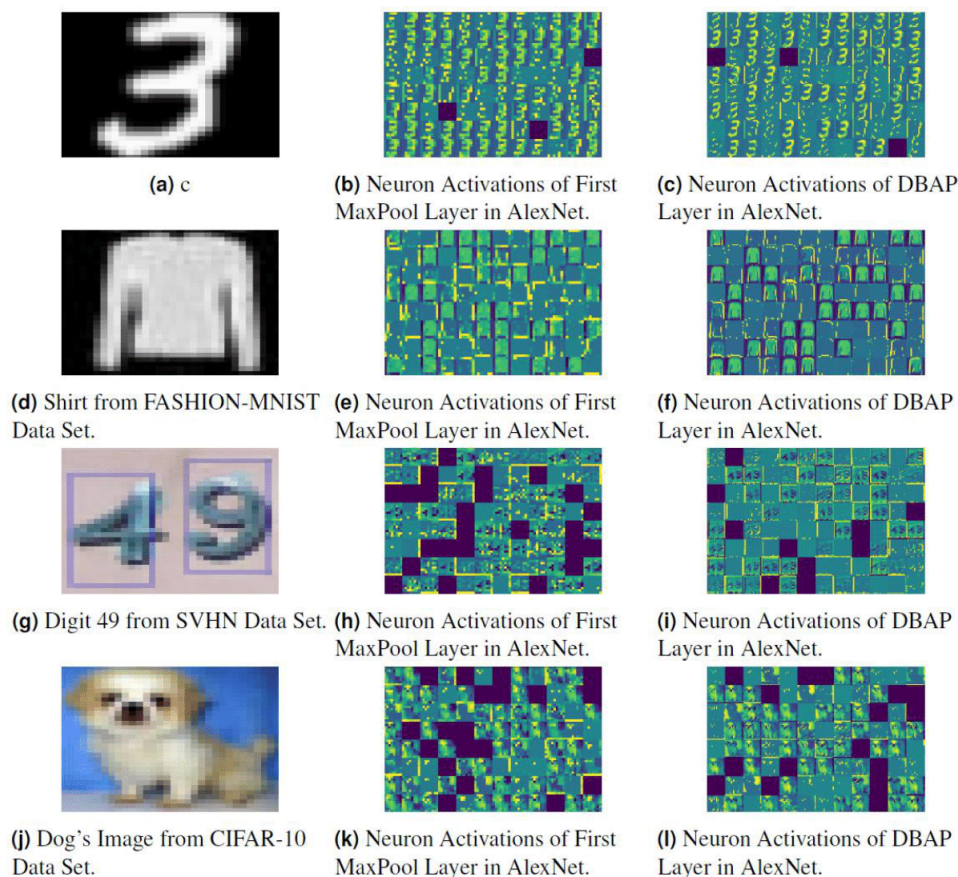


**Figure 6.** Visualising the response of neurons in MaxPool layer and DBAP layer with baseline AlexNet and AlexNet with DBAP layer respectively. AlexNet uses 96 filters/kernels of size  $3 \times 3$ . in the first MaxPool layer and one can see that DBAP layer retains most of the input image's information as compared to the MaxPool layer.

#### 262 5.4 Visual Diagnostics Used to Evaluate Feature Information Quality

263 In order to understand how the input image is transformed by each intermediate layer of CNN, the  
 264 activations of neurons in pooling layer and DBAP layer are visualised. The feature maps are visualised  
 265 in three dimensions: Width, height and depth (channels). Since each channel encodes independent  
 266 information, one appropriate way to visualise these features is to plot 2D images of each channel  
 267 separately. Given our existing knowledge of deep neural models, the initial layers act as edge detectors  
 268 and retain most of the information of the input image. As we go higher, the activations become increasingly  
 269 abstract and less interpretable visually. The sparsity of activations increases with the depth of the layer, i.e.  
 270 more and more filters would go blank and the pattern encoded in the image could not be seen. We thus  
 271 expect that the activation filters of DBAP layer should be more interpretable and semantically meaningful  
 272 given the input image, model is observing.

#### 273 5.5 Implementation Details for Model Training

274 In this section, we discuss how the choice of different hyper-parameters such as kernel's filter size, batch  
 275 size, learning rate, epochs and optimisation algorithm is made to train the CNN models for each specific  
 276 data set on board. To decide on this, we first divide our data set into three different subsets: Train set,  
 277 cross validated set and test set. For the selected benchmark data sets discussed in Section 5.1, the train and  
 278 test set segregation exists already. The cross validated set is obtained by splitting the train data randomly  
 279 in 80:20 ratio, reserving 20% of the data points for the validation purpose and 80% of the train instances

280 for the training objective. When deciding optimal values of epochs, learning rate, batch size, filter size  
 281 and optimiser, 80% of these train instances are used to train both the neural models and their performance  
 282 is judged on the 20% validation set examples. Once optimal values of these parameters are decided, the  
 283 entire train set is used to train both the neural models and their performance is assessed on the available  
 284 test sets. The train time of the proposed CNN models varies within this wall clock range [2.5, 3 hours],  
 285 when run on Google Colab.

286 In order to assess if the model is overfitting with the chosen set of parameters or hyper-parameters,  
 287 the performance is compared on train and validation sets in Figure 3 and 4. If the model behaves very  
 288 well on the train set but fails to classify examples from the validation set by a huge margin, it means that  
 289 it is overfitting and shall not perform well on unseen test examples. Some of the ways in which model  
 290 overfitting could be avoided are: Cross-validation, usage of more train data, early stopping, regularisation  
 291 and removal of features. We have regularised the models which were overfitting with the help of the  
 292 validation set.

### 293 **5.5.1 Impact of Learning Rate and Epochs on Model Training**

294 The training of CNN depends largely on the learning rate and number of epochs used to learn the  
 295 parameters. The learning rate hyperparameter controls the speed at which the model learns. For small  
 296 learning rate, large number of epochs are required to train the model, whereas for large learning rate,  
 297 small number of epochs are needed to navigate in the parameter space of the neural model. A learning rate  
 298 that is too large can cause the model to converge too quick to a sub-optimal solution, whereas a learning  
 299 rate that is too small can cause the learning process to become very slow. Therefore, it is advised to  
 300 choose a value that is neither too large nor too small. Its value typically ranges between 0 and 1. We have  
 301 configured the best value for learning rate using grid search method. Grid search involves picking values  
 302 approximately on a logarithmic scale within the set range:  $\{10^{-4}, 10^{-3}, 10^{-2}, 10^{-1}, 10^0\}$ , and observes  
 303 the validation loss while keeping the value of epochs fixed. We confined the value of epochs to 50 and  
 304 observed the impact of changing learning rate on the validation set. Figures 3 and 4 demonstrate the  
 305 accuracy of LeNet and AlexNet models, when the learning rate was fixed at 0.01 and the model was run  
 306 for 50 epochs. Since the validation error is lowest when  $\eta = 0.01$ , and the gap between the train and  
 307 validation error is not significantly large, the model does not tend to overfit and 0.01 turns out to be the  
 308 most suitable value for learning rate.

### 309 **5.5.2 Impact of Batch Size on Model Training**

310 Batch size is also an important hyperparameter that impacts a model's performance. Table 1 shows the  
 311 best batch size for each data set when learning rate and epochs are fixed at 0.01 and 50 respectively using  
 312 the AlexNet architecture. A similar comparison was also performed for LeNet architecture and best  
 313 batch sizes for MNIST, Fashion-MNIST, SVHN and CIFAR-10 were chosen as 128, 128, 128 and 256  
 314 respectively.

**Table 1.** Overall Accuracy of the Proposed System on the Validation Set Using Different Batch Sizes.

Data Sets	Batch Sizes		
	64	128	256
MNIST	99.1 %	98.6 %	<b>99.5 %</b>
FASHION-MNIST	90.8 %	90.2 %	<b>91.8 %</b>
SVHN	<b>94.4 %</b>	92.5 %	93.1 %
CIFAR-10	78.3 %	78.8 %	<b>80.6 %</b>

### 315 **5.5.3 Impact of Optimisers**

316 In order to update the parameters of convolutional neural network, different popular optimisers such as  
 317 stochastic gradient decent (SGD), adam (Kingma and Ba, 2014) and ADADELTA (Zeiler, 2012), were  
 318 tested and evaluated on the validated set. Table 2 highlights the accuracy of AlexNet with DBAP layer  
 319 when different types of optimisers were used. We observe that for MNIST data set, Adadelata optimiser  
 320 shows the best results, whereas for FASHION-MNIST, SVHN and CIFAR-10 data sets, SGD optimiser  
 321 outperforms the remaining optimisation algorithms. A similar analysis was also performed for LeNet  
 322 with DBAP layer and best optimisers were selected accordingly.

**Table 2.** Overall Accuracy of the Proposed System on the Validation Set Using Different Types of Optimisers for Training AlexNet.

Data Sets	Optimisers		
	SGD	Adam	AdaDelta
MNIST	98.1 %	98.6 %	<b>99.5 %</b>
FASHION-MNIST	<b>91.5 %</b>	90.6 %	90.1 %
SVHN	<b>93.2 %</b>	92.1 %	91.7 %
CIFAR-10	<b>78.2 %</b>	78.1 %	77.6 %

#### 323 5.5.4 Impact of LBP Filter Size on CNN

324 We have also assessed different kernel sizes used in DBAP layer to capture local features of images that  
 325 add to the discriminative ability of neural models. Table 3 shows that  $3 \times 3$  window gives best accuracy on the validation set in comparison to larger size filters on all the data sets.

**Table 3.** Classification Accuracy on the Validation Set of Four Benchmark Data Sets with Varying Filter Size in DBAP Layer of AlexNet.

Data Sets	Window Size		
	$3 \times 3$	$5 \times 5$	$7 \times 7$
MNIST	99.5%	97.1%	96.1%
F-MNIST	91.8%	88.9%	88.2%
SVHN	94.4%	93.2%	91.5%
CIFAR-10	80.6%	74.5%	76.2%

326

**Table 4.** Classification accuracy yielded by LeNet and AlexNet (in %) after incorporation of DBAP layer. The classifier used is softmax by both the models. One can observe that the results are better than those achieved by the baseline models and competitive to the discrimination results of other popular deep models.

Data Sets	Baseline LeNet	LeNet with DBAP	Baseline AlexNet	AlexNet with DBAP	LBP Features with $k$ -NN	LBP Features with SVM	MobileNet (Howard et al., 2017)	GoogLeNet (Szegedy et al., 2015)	LBCNN (Juefei et al., 2017)
MNIST	99.0 %	<b>99.1 %</b>	99.2 %	<b>99.5 %</b>	88.7 %	83.7 %	94.59 %	97.98 %	99.51 %
F-MNIST	89.8 %	<b>91.0 %</b>	90.5 %	<b>91.5 %</b>	78.3 %	73.5 %	-	93.5 %	-
SVHN	86.7 %	<b>88.3 %</b>	87.3 %	<b>94.4 %</b>	29.6 %	25.9 %	90.8 %	92.3 %	94.50 %
CIFAR-10	72.3 %	<b>74.8 %</b>	73.7 %	<b>80.6 %</b>	28.3 %	27.6 %	65.6 %	76.5 %	92.99 %

**Table 5.** Accuracy of SVM classifier on DBAP features derived from pre-trained LeNet with DBAP layer. The DBAP features show better classification results than the MaxPool features in LeNet. The fully connected (FC) layers of LeNet with DBAP also tend to show better discrimination ability as compared to FC layer features extracted from regular LeNet on all benchmark data sets.

Data Sets	MaxPool Layer (Layer 2)	DBAP Layer (Layer 2)	FC Layer from LeNet (Layer 7)	FC Layer from LeNet with DBAP (Layer 7)
MNIST	98.1% (C=100)	<b>98.3% (C=100)</b>	98.4% (C=100)	<b>99.0% (C=1)</b>
F-MNIST	88.6% (C=100)	<b>89.0% (C=100)</b>	90.4% (C=100)	<b>91.3% (C=100)</b>
SVHN	81.2% (C=10)	<b>82.0% (C=10)</b>	83.9% (C=10)	<b>86.8% (C=100)</b>
CIFAR-10	52.1% (C=10)	<b>52.9% (C=100)</b>	57.4% (C=10)	<b>65.3% (C=10)</b>

#### 327 5.6 Model Testing

328 After fine tuning the neural models with optimal parameters and hyperparameters, we next compute the  
 329 classification performance of the proposed model on unseen test examples of each standard data set.

**Table 6.** Accuracy of SVM classifier on DBAP features derived from pre-trained AlexNet with DBAP layer. The classification results are better than the results obtained by MaxPool features derived from a regular AlexNet. The inclusion of DBAP layer also shows better FC features from the model giving better classification results in comparison to the FC features from regular AlexNet model.

Data Sets	MaxPool Layer (Layer 2)	DBAP Layer (Layer 2)	FC Layer from AlexNet (Layer 11)	FC Layer from AlexNet with DBAP (Layer 11)
MNIST	95.1% (C=100)	<b>98.0%</b> (C=100)	99.1% (C=100)	<b>99.2%</b> (C=0.01)
F-MNIST	89.8% (C=1)	<b>90.4%</b> (C=1)	90.9% (C=100)	<b>91.4%</b> (C=1)
SVHN	80.1% (C=1)	<b>80.2%</b> (C=100)	89.0% (C=1)	<b>94.5%</b> (C=10)
CIFAR-10	60.3% (C=100)	<b>63.3%</b> (C=100)	80.3% (C=100)	<b>84.3%</b> (C=100)

**Table 7.** Accuracy of  $k$ -NN classifier on DBAP features derived from pre-trained LeNet with DBAP layer. The results achieved are better than the ones obtained by MaxPool layer in a regular LeNet. The inclusion of DBAP layer also improves the FC features for discrimination task.

Data Sets	MaxPool Layer (Layer 2)	DBAP Layer (Layer 2)	FC Layer from LeNet (Layer7)	FC Layer from LeNet with DBAP (Layer 7)
MNIST	97.4% (k=2)	<b>97.7%</b> (k=2)	98.8% (k=2)	<b>99.0%</b> (k=2)
F-MNIST	77.6% (k=2)	<b>78.2%</b> (k=2)	84.6% (k=2)	<b>91.2%</b> (k=16)
SVHN	77.2% (k=32)	<b>78.6%</b> (k=32)	85.9% (k=2)	<b>86.6%</b> (k=8)
CIFAR-10	56.0% (k=2)	<b>59.7%</b> (k=9)	63.8% (k=4)	<b>65.0%</b> (k=27)

**Table 8.** Accuracy of  $k$ -NN classifier on DBAP features derived from pre-trained AlexNet with DBAP layer. The classification results achieved are better than those obtained by MaxPool features derived from regular AlexNet. The inclusion of DBAP layer also improves the discrimination quality of FC features in AlexNet with DBAP layer.

Data Sets	MaxPool Layer (Layer 2)	DBAP Layer (Layer 2)	FC Layer from AlexNet (Layer 11)	FC Layer from AlexNet with DBAP (Layer 11)
MNIST	97.9% (k=2)	<b>98.0%</b> (k=2)	98.7% (k=2)	<b>99.1%</b> (k=4)
F-MNIST	83.1% (k=2)	<b>87.2%</b> (k=2)	88.6% (k=2)	<b>89.5%</b> (k=16)
SVHN	66.0% (k=2)	<b>68.4%</b> (k=2)	88.0% (k=2)	<b>94.4%</b> (k=16)
CIFAR-10	52.7% (k=32)	<b>53.6%</b> (k=41)	68.9% (k=16)	<b>83.7%</b> (k=16)

**Table 9.** Comparison of the number of trainable parameters in regular LeNet, LeNet with DBAP layer, regular AlexNet and AlexNet with DBAP layer.

Layer Name	Tensor Size	Number of Parameters
Input Image	$28 \times 28 \times 1$	0
Conv-1	$26 \times 26 \times 6$	60
DBAP	$26 \times 26 \times 6$	0
Conv-2	$24 \times 24 \times 16$	880
MaxPool-2	$12 \times 12 \times 16$	0
FC-1	$120 \times 1$	276,600
FC-2	$84 \times 1$	10,164
FC-3	$10 \times 1$	850
Output	$10 \times 1$	0
<b>Total</b>		<b>288,554 (~ 0.28M)</b>

**(b)** Architecture of LeNet with DBAP Layer.

Layer Name	Tensor Size	Number of Parameters
Input Image	$28 \times 28 \times 1$	0
Conv-1	$14 \times 14 \times 96$	960
MaxPool-1	$7 \times 7 \times 96$	0
Conv-2	$7 \times 7 \times 256$	614,656
MaxPool-2	$3 \times 3 \times 256$	0
Conv-3	$3 \times 3 \times 384$	885,120
Conv-4	$3 \times 3 \times 384$	1,327,488
Conv-5	$3 \times 3 \times 256$	884,992
MaxPool-3	$1 \times 1 \times 256$	0
FC-1	$4096 \times 1$	1,052,672
FC-2	$4096 \times 1$	16,781,312
FC-3	$10 \times 1$	40,970
Output	$10 \times 1$	0
<b>Total</b>		<b>21,588,170 (~ 21M)</b>

**(c)** AlexNet Architecture

Layer Name	Tensor Size	Number of Parameters
Input Image	$28 \times 28 \times 1$	0
Conv-1	$14 \times 14 \times 96$	960
DBAP	$14 \times 14 \times 96$	0
Conv-2	$14 \times 14 \times 256$	614,656
MaxPool-2	$6 \times 6 \times 256$	0
Conv-3	$6 \times 6 \times 384$	885,120
Conv-4	$6 \times 6 \times 384$	1,327,488
Conv-5	$6 \times 6 \times 256$	884,992
MaxPool-3	$2 \times 2 \times 256$	0
FC-1	$4096 \times 1$	41,98,400
FC-2	$4096 \times 1$	16,781,312
FC-3	$10 \times 1$	40,970
Output	$10 \times 1$	0
<b>Total</b>		<b>24,733,898 (~ 24M)</b>

**(d)** Architecture of AlexNet with DBAP Layer.

### 330 **5.6.1 Analysis of CNN Model with DBAP Layer as a Classifier**

331 When deploying CNN as a classifier, the test data is passed to the trained CNN model with DBAP layer,  
 332 whose last layer consisting of softmax units is utilised for object categorisation. The discrimination  
 333 performance of the model is assessed with the help of following evaluation metrics: Accuracy, precision,  
 334 recall, F1-score, and area under the curve (AUC), discussed in Section 5.3 and 7. Table 4 shows  
 335 improvement in the discrimination performance yielded by the proposed approach in comparison to the  
 336 baseline AlexNet and LeNet architectures on four different benchmark data sets. We have also compared  
 337 our results with local binary convolutional neural network (LBCNN) that offers to provide an alternative  
 338 to standard convolutional layers in the convolutional neural network (Juefei et al., 2017), GoogleNet (also  
 339 known as Inception V1) (Szegedy et al., 2015) and MobileNet (Howard et al., 2017). GoogleNet is a  
 340 22-layer CNN inspired by LeNet, whereas MobileNet is an efficient CNN architecture with 17 layers  
 341 streamlined for mobile applications. We observe that the classification performance of the proposed  
 342 model with DBAP layer is competitive to the state of the art results shown by ultra deep convolutional  
 343 neural models. The precision, recall and F1 scores of the proposed model further reassure the precision  
 344 and discrimination power of the proposed deep model for unseen test examples.

345 In Table 4, one may observe that unlike other data sets, the classification results of DBAP features  
 346 on CIFAR-10 data set are a lot worse in comparison to LBCNN (Juefei et al., 2017). This is because  
 347 the images in CIFAR-10 possess natural objects with rich textures as compared to the hand written digit  
 348 images present in other data sets. For this reason, LBCNN works exceptionally better on CIFAR-10 in  
 349 comparison to AlexNet with DBAP features. Also LBCNN replaces all convolutional layers of AlexNet  
 350 with LBP inspired layers which is popular for extracting discriminative texture descriptors, whereas our  
 351 proposed model only replaces the first MaxPooling layer with LBP inspired feature detectors, hence the  
 352 performance gap is higher in contrast. Similar impact in performance could also be observed in area under  
 353 the curve graphs shown in the supplementary section.

354 We have conducted experiments to compare the discrimination power of LBP operator with DBAP  
 355 features in Table 4. The classifiers used for the purpose are k-NN and SVM. One can observe that  
 356 LBP operator on its own does not yield as good classification results as the DBAP layer introduced in  
 357 LeNet and AlexNet architectures. The open source code developed for these experiments is available at  
 358 :<https://github.com/shakeel0232/DBAP-CNN>.

### 359 **5.6.2 Analysis of CNN Model with DBAP Layer as a Feature Extractor**

360 In order to assess the discrimination power of features learned by DBAP layer, we have also checked  
361 their accuracy with simple off the shelf classifiers like  $k$ -nearest neighbour ( $k$ -NN) and support vector  
362 machines (SVM). We selected pre-trained CNN models with and without DBAP layer to extract features  
363 for image classification task. The results shown in Tables 5, 6, 7 and 8 demonstrate that DBAP layer  
364 can serve as a competitive feature extractor in comparison to the intermediate layer features such as  
365 MaxPooling layer of AlexNet and LeNet. For SVM classifier, the optimal value of parameter  $C$  is searched  
366 via grid-search method on the validation set and shown against each data set in the tables. Similarly, for  
367  $k$ -nearest neighbour ( $k$ -NN), the optimal value of  $k$  is searched using the validation set and then used  
368 for the test data in each benchmark data set. The empirical results reveal that DBAP features could be  
369 used as readily available features from a pre-trained model for applications where quick retrieval and  
370 classification results are required.

371 We have also assessed the impact of DBAP layer on FC layer features. The fully connected (FC)  
372 layers are known to retain better discrimination power for classification tasks, however with the inclusion  
373 of DBAP layer, their ability to classify objects is further improved as can be seen in the last two columns  
374 of Tables 5, 6, 7 and 8 .

### 375 **5.6.3 Statistical Significance of Models**

376 We have also applied hypothesis testing to estimate the statistical significance of the proposed models.  
377 Statistical tests help us identify the behaviour of models if the test set changes. Since our data sets are  
378 standardised, we assume a normal distribution of features and have applied McNemar's test or  $5 \times 2$   
379 cross-validation with a modified paired Student  $t$ -test. The null hypothesis assumes that the two samples  
380 came from the same distribution. In contrast, the alternative hypothesis assumes that the samples came  
381 from two different distributions and hence there is a difference between the tested models or classifiers.  
382 With 0.05 level of confidence/significance, the  $p$  values attained for LeNet with DBAP layer and AlexNet  
383 with DBAP layer models are 0.007 and 0.011 respectively. In both the cases,  $p < 0.05$ , shows the samples  
384 generated from the proposed architectures are statistically different from the ones without DBAP layer.

### 385 **5.7 Visualisation of Filters**

386 We have also visualised the mid-level features learned by DBAP layer and compared them with the  
387 features learned by max-pooling layers used in classical CNN architectures. Figures 5 and 6 demonstrate  
388 the improvement in visual representation of intermediate features learned by the two CNN architectures  
389 in comparison to their baseline counterparts with maxpooling layer. One can observe that DBAP layer  
390 learns semantically better features from the input images as compared to the maxpooling layer used in  
391 classical LeNet and AlexNet architectures. As we go higher in the model hierarchy, the filters become  
392 more abstract and sparsity of the activations increases, i.e. the filters become more blank and the pattern  
393 encoded by the image is not showcased by the filter (François, 2017).

394 Improving the visualisation strength of neural models can help us explore and understand the black  
395 box learning behaviour of deep models. Better visualisation can serve as a great diagnostic tool (Liu et al.,  
396 2019) for observing the evolution of features during model training and diagnose potential problems with  
397 the model via online/offline feature representations. This facilitates the researchers to fix their training  
398 practices and find models that can outperform an existing successful deep model. For example, the  
399 deconvolutional technique proposed for visualising the hidden layer features suggested an architectural  
400 change of smaller convolutional filters that lead to state of the art performance on the ImageNet benchmark  
401 in 2013 (Zeiler and Fergus, 2014).

### 402 **5.8 Proposed Model's Complexity**

403 We next compare the count of trainable parameters in LeNet and AlexNet containing DBAP layers with  
404 their baseline counter parts in Table 9. The total number of CNN parameters are the sum of all its weights  
405 and biases connecting the convolutional, input, output and fully connected layers. The pooling layers  
406 in the architecture do not contribute to the count of model parameters as they contain hyper-parameters  
407 such as pool size, stride, and padding which do not need to be learned during the training phase. The  
408 number of model parameters before the advent of DBAP layer remain fixed. However, when we replace  
409 the first pooling layer with DBAP layer, the output tensor of Layer 2 is not down sampled as it does  
410 in regular LeNet and AlexNet architectures, rather the tensor scale remains the same as its input (i.e.  
411  $26 \times 26 \times 6$  for LeNet and  $14 \times 14 \times 96$  for AlexNet). This impacts the size of the kernel in the following

convolutional layer, and the effect is carried out forward to the next maxpooling and fully connected layers. Overall, there is an increase of 380.33% in LeNet parameters and an increase of 14.57% in AlexNet model parameters with the inclusion of DBAP layer.

Keeping in view the size of model parameters, the proposed model is not well suited for resource constrained environments, where storage and computation of large number of parameters becomes a bottleneck. However, it offers two fold advantage in comparison to the state of the art models: (1) Effective intermediate feature visualisation power and (2) competitive discrimination performance as a feature extractor and classifier. Models such as LBCNN (Juefei et al., 2017) propose to use a compact neural model whose convolutional layers are all replaced by LBP operator. This move reduces the number of learnable parameters massively to around 0.352million, thus making it very suitable for resource constrained environments.

## 6 CONCLUSION & FUTURE WORK

In this paper, we propose to induce discrimination into the intermediate layers of the convolutional neural network by introducing a novel local binary pattern layer that can serve as a replacement of the first standard maxpooling layer used at early stage of feature learning in the convolutional neural network. The empirical results on benchmark data sets as well as the visual feature maps of intermediate layers demonstrate the strength of the proposed idea to learn more discriminative features without building ultra deep models. Our experiments reveal that the proposed approach can strengthen the discriminative power of mid-level features as well as high level features learned by fully connected (FC) layers of convolutional neural network. The experiments with simple classifier like  $k$ -NN and popular industry classifier like SVM, suggest the use of intermediate DBAP layer and its following fully connected layers in the deep learning pipeline for off-line feature extraction and classification tasks.

In future, we aim to improve the training complexity of the proposed approach by reducing the number of learnable parameters for model training. In this regard, we shall explore sparsity in the neural connections to adopt suitable regularisation technique for fast model learning.

## 7 SUPPLEMENTARY

The supplementary section shows some additional results to support reproducible research and make the main text more readable and understandable. We have shown precision, recall and F1-score of LeNet and Alexnet models along with their improved counterparts in Tables 10 and 11. These evaluation metrics in combination with the accuracy show how good the proposed models are in comparison to their baseline models.

One can also observe the area under the curve (AUC) for the developed classifiers in Figures 7, 8, 9 and 10. AUC ranges between 0 and 1. Higher the AUC, better the model is at predicting classes correctly as positive and negative, significantly above the random chance. AUC is good at catching the performance of models when the class distribution is skewed. We observe that with the addition of DBAP layer in CNN architecture, AUC in ROC either increases or remains the same as shown in few cases.

**Table 10.** Precision, Recall and F1-Score of LeNet and LeNet with DBAP Layer Using Softmax Classifier.

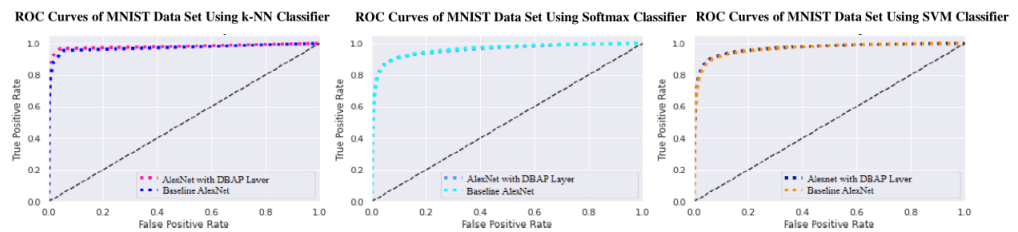
Data Sets	LeNet			LeNet-with-DBAP		
	Precision	Recall	F1-Score	Precision	Recall	F1-Score
MNIST	99 %	99 %	99 %	99 %	99 %	99 %
FASHION-MNIST	90 %	90 %	90 %	91 %	91 %	91 %
SVHN	86 %	85 %	86 %	88 %	87 %	87 %
CIFAR-10	72 %	72 %	72 %	74 %	75 %	74 %

## REFERENCES

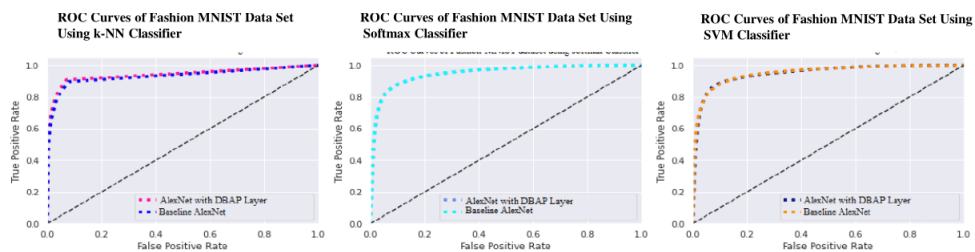
(2019). Google Colab Free Gpu Tutorial. <https://medium.com/deep-learning-turkey>. Accessed: 02-07-2019.

**Table 11.** Precision, Recall and F1-Score of AlexNet and AlexNet with DBAP Layer Using Softmax Classifier.

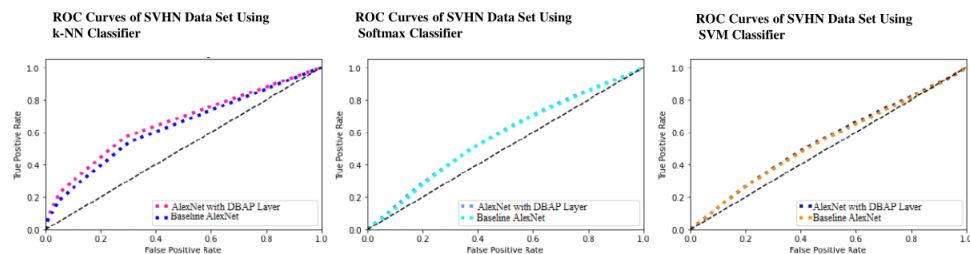
Data Sets	AlexNet			AlexNet-with-DBAP		
	Precision	Recall	F1-Score	Precision	Recall	F1-Score
MNIST	99 %	99 %	99 %	100 %	99 %	100 %
FASHION-MNIST	91 %	91 %	91 %	91 %	91 %	91 %
SVHN	90 %	90 %	90 %	94 %	94 %	94 %
CIFAR-10	71 %	72 %	71 %	77 %	78 %	77 %



(a) AUC with Baseline AlexNet=0.97 & AlexNet with DBAP Layer is 0.98. (b) AUC with Baseline AlexNet & AlexNet with DBAP Layer= 0.96. AlexNet with DBAP Layer= 0.97. (c) AUC with Baseline AlexNet & AlexNet with DBAP Layer= 0.97. AlexNet with DBAP Layer= 0.97.

**Figure 7.** ROC Curve of k-NN, Softmax and SVM Classifiers on MNIST Data Set.

(a) AUC with Baseline AlexNet =0.93 & AlexNet with DBAP Layer= 0.94. (b) AUC with Baseline AlexNet & AlexNet with DBAP Layer= 0.95. AlexNet with DBAP Layer= 0.95. (c) AUC with Baseline AlexNet & AlexNet with DBAP Layer= 0.95. AlexNet with DBAP Layer= 0.95.

**Figure 8.** ROC Curve of k-NN, Softmax and SVM Classifiers on Fashion MNIST Data Set.

(a) AUC with Baseline AlexNet =0.63 & AlexNet with DBAP Layer= 0.66. (b) AUC with Baseline AlexNet=0.57 & AlexNet with DBAP Layer= 0.58. (c) AUC with Baseline AlexNet=0.54 & AlexNet with DBAP Layer= 0.55.

**Figure 9.** ROC Curve of k-NN, Softmax and SVM Classifiers on SVHN Data Set.

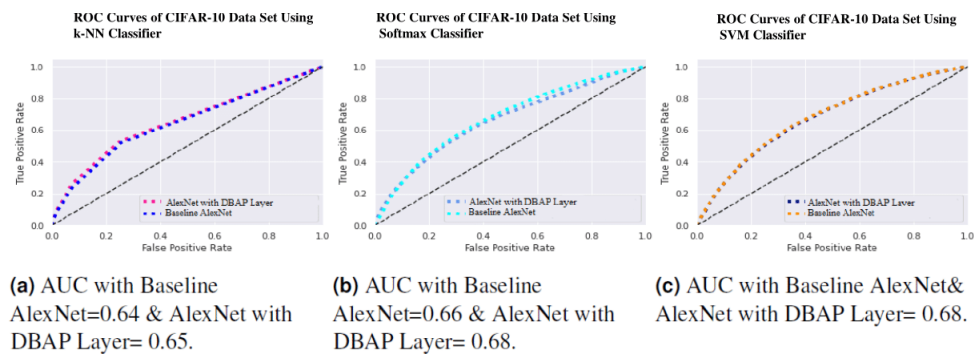


**Figure 10.** ROC Curve of k-NN, Softmax and SVM Classifiers on CIFAR-10 Data Set.

- 451 Babenko, A. and Lempitsky, V. (2015). Aggregating Local Deep Features For Image Retrieval. In  
 452 *Proceedings of IEEE ICCV*, pages 1269–1277.
- 453 Bau, D., Zhu, J., Strobel, H., Zhou, B., Tenenbaum, J., Freeman, W., and Torralba, A. (2019). Visualizing  
 454 and Understanding Generative Adversarial Networks. *arXiv preprint arXiv:1901.09887*.
- 455 Bengio, Y., Courville, A., and Vincent, P. (2013a). Representation Learning: A Review and New  
 456 Perspectives. *PAMI*, 35(8):1798–1828.
- 457 Bengio, Y., Courville, A., and Vincent, P. (2013b). Representation Learning: A Review and New  
 458 Perspectives. *IEEE PAMI*, 35(8):1798–1828.
- 459 Chollet, F. et al. (2015). Keras.
- 460 Cimpoi, M., Maji, S., and Vedaldi, A. (2015). Deep Filter Banks For Texture Recognition and Segmenta-  
 461 tion. In *CVPR*, pages 3828–3836.
- 462 D. Cashman, G. Patterson, A. M. and Chang, R. (2017). RNNbow: Visualizing Learning via Back-  
 463 propagation Gradients in Recurrent Neural Networks. In *Workshop on Visual Analytics for Deep  
 464 Learning*.
- 465 Deng, J., Dong, W., Socher, R., Li, L.-J., Li, K., and Fei-Fei, L. (2009). Imagenet: A Large-Scale  
 466 Hierarchical Image Database. In *IEEE Conf. on CVPR*, pages 248–255. IEEE.
- 467 Do, D. T., Le, T. Q. T., and Le, N. Q. K. (2020). Using Deep Neural Networks and Biological Subwords  
 468 to Detect Protein S-sulfenylation Sites. *Briefings in Bioinformatics*.
- 469 François, C. (2017). Deep Learning with Python.
- 470 Gagne, D., Haupt, E., Nychka, D., and Thompson, G. (2019). Interpretable Deep Learning For Spatial  
 471 Analysis of Severe Hailstorms. *Monthly Weather Review*, (2019).
- 472 Girshick, R., Donahue, J., Darrell, T., and Malik, J. (2014). Rich Feature Hierarchies for Accurate Object  
 473 Detection and Semantic Segmentation. In *Proceedings of the IEEE Conf. on CVPR*, pages 580–587.
- 474 Goodfellow, I., Bengio, Y., and Courville, A. (2016). *Deep Learning*. MIT Press.
- 475 Hazard, C., Fusting, C., Resnick, M., Auerbach, M., Meehan, M., and Korobov, V. (2019). Natively  
 476 Interpretable Machine Learning and Artificial Intelligence: Preliminary Results and Future Directions.  
 477 *arXiv preprint arXiv:1901.00246*.
- 478 He, K., Zhang, X., Ren, S., and Sun, J. (2014). Spatial Pyramid Pooling in Deep Convolutional Networks  
 479 for Visual Recognition. In *ECCV*, pages 346–361. Springer.
- 480 He, K., Zhang, X., Ren, S., and Sun, J. (2015). Delving Deep into Rectifiers: Surpassing Human-Level  
 481 Performance On Imagenet Classification. In *Proceedings of IEEE ICCV*, pages 1026–1034.
- 482 He, K., Zhang, X., Ren, S., and Sun, J. (2016). Deep Residual Learning for Image Recognition. In  
 483 *Proceedings of IEEE CVPR*, pages 770–778.
- 484 Hinton, G., Deng, L., Yu, D., Dahl, G., Mohamed, A.-r., Jaitly, N., Senior, A., Vanhoucke, V., Nguyen, P.,  
 485 Kingsbury, B., et al. (2012). Deep Neural Networks For Acoustic Modeling In Speech Recognition.  
 486 *IEEE Signal Processing Magazine*, 29.
- 487 Hohman, F., Kahng, M., Pienta, R., and Chau, D. H. (2018). Visual Analytics in Deep Learning:  
 488 An Interrogative Survey for the Next Frontiers. *IEEE Transactions on Visualization and Computer  
 489 Graphics*, 25(8):2674–2693.
- 490 Howard, A., Zhu, M., Chen, B., Kalenichenko, D., Wang, W., Weyand, T., Andreetto, M., and Adam, H.

- 491 (2017). Mobilenets: Efficient Convolutional Neural Networks for Mobile Vision Applications. *arXiv*  
492 *preprint arXiv:1704.04861*.
- 493 Juefei, F., Boddeti, N., and Savvides, M. (2017). Local Binary Convolutional Neural Networks. In *IEEE*  
494 *Conference on CVPR*, volume 1.
- 495 Kingma, D. and Ba, J. (2014). Adam: A Method For Stochastic Optimization. *arXiv preprint*  
496 *arXiv:1412.6980*.
- 497 Krizhevsky, A. and Hinton, G. (2009). Learning Multiple Layers Of Features From Tiny Images. Technical  
498 Report 1(4), University of Toronto.
- 499 Krizhevsky, A., Nair, V., and Hinton, G. (2014). The Cifar-10 Dataset. *online: <http://www.cs.toronto.edu/kriz/cifar.html>*.
- 500 Krizhevsky, A., Sutskever, I., and Hinton, G. (2012). Imagenet Classification With Deep Convolutional  
501 Neural Networks. In *Advances in NIPS*, pages 1097–1105.
- 502 Kumar, R., Banerjee, A., and Vemuri, B. (2009). Voltterrafaces:Discriminant Analysis Using Volterra  
503 Kernels. pages 150–155. IEEE.
- 504 Kumar, R., Banerjee, A., Vemuri, B., and Pfister, H. (2012). Trainable Convolution Filters and Their  
505 Application To Face Recognition. *PAMI*, 34(7):1423–1436.
- 506 Le, N. Q. K. (2019). Fertility-GRU: Identifying Fertility-Related Proteins by Incorporating Deep-gated  
507 Recurrent Units and Original Position-Specific Scoring Matrix Profiles. *Journal of proteome research*,  
508 18(9):3503–3511.
- 509 Le, N. Q. K. and Nguyen, V.-N. (2019). SNARE-CNN: A 2D Convolutional Neural network Architecture  
510 to Identify SNARE Proteins from High-throughput Sequencing Data. *PeerJ Computer Science*, 5:e177.
- 511 LeCun, Y., Bengio, Y., and Hinton, G. (2015). Deep Learning. *Nature*, 521(7553):436.
- 512 LeCun, Y., Boser, B., Denker, J., Henderson, D., Howard, R., Hubbard, W., and Jackel, L. (1989).  
513 Backpropagation Applied to Handwritten Zip Code Recognition. *NC*, 1(4):541–551.
- 514 LeCun, Y., Boser, B., Denker, J., Henderson, D., Howard, R., Hubbard, W., and Jackel, L. (1990).  
515 Handwritten Digit Recognition With A Back-propagation Network. In *NIPS*, pages 396–404.
- 516 LeCun, Y., Bottou, L., Bengio, Y., Haffner, P., et al. (1998). Gradient-Based Learning Applied To  
517 Document Recognition. *IEEE*, 86:2278–2324.
- 518 Liu, G., Zeng, H., and Gifford, D. (2019). Visualizing Complex Feature Interactions and Feature Sharing  
519 in Genomic Deep Neural Networks. *BMC Bioinformatics*, 20(1):1–14.
- 520 Liu, L., Shen, C., and van Hengel, A. (2015). The Treasure Beneath Convolutional Layers: Cross-  
521 convolutional-layer Pooling For Image Classification. In *Proceedings of IEEE Conference on CVPR*,  
522 pages 4749–4757.
- 523 Liu, L., Shen, C., and van Hengel, A. (2017a). Cross-Convolutional-Layer Pooling For Image Recognition.  
524 *IEEE Transactions on PAMI*, 39(11):2305–2313.
- 525 Liu, L., Wang, P., Shen, C., Wang, L., Hengel, A., Wang, C., and Shen, H. (2017b). Compositional Model  
526 Based Fisher Vector Coding For Image Classification. *PAMI*, 39:2335–2348.
- 527 Masumoto, H., Tabuchi, H., Nakakura, S., Ohsugi, H., Enno, H., Ishitobi, N., Ohsugi, E., and Mitamura,  
528 Y. (2019). Accuracy of a Deep Convolutional Neural Network in Detection of Retinitis Pigmentosa on  
529 Ultrawide-field Images. *PeerJ*, 7:e6900.
- 530 Mordvintsev, A., Olah, C., and Tyka, M. (2015). Inceptionism: Going Deeper into Neural Net.
- 531 Netzer, Y., Wang, T., Coates, A., Bissacco, A., Wu, B., and Ng, A. (2011). Reading Digits In Natural  
532 Images With Unsupervised Feature Learning. In *NIPS*, volume 2011, page 5.
- 533 Ng, J., Yang, F., and Davis, L. (2015). Exploiting Local Features from Deep Networks for Image Retrieval.  
534 In *CVPR Workshop*.
- 535 Ojala, T., Pietikainen, M., and Harwood, D. (1994). Performance Evaluation of Texture Measures with  
536 Classification Based on Kullback Discrimination of Distributions. In *Pattern Recognition, Conference*  
537 *A: Computer Vision & Image Processing*, volume 1, pages 582–585. IEEE.
- 538 Poole, B., Lahiri, S., Raghu, M., Sohl, J., and Ganguli, S. (2016). Exponential Expressivity In Deep  
539 Neural Networks Through Transient Chaos. In *NIPS*, pages 3360–3368.
- 540 Raghu, M., Poole, B., Kleinberg, J., Ganguli, S., and Dickstein, S. (2017). On The Expressive Power Of  
541 Deep Neural Networks. In *Proceedings of Machine Learning*, pages 2847–2854. JMLR.
- 542 Ren, Z., Kong, Q., Han, J., Plumbley, M., and Schuller, B. W. (2019). Attention-Based Atrous Con-  
543 volutional Neural Networks: Visualisation And Understanding Perspectives Of Acoustic Scenes. In  
544 *Proceedings of IEEE ICASSP*.
- 545

- 546 Sabour, S., Frosst, N., and Hinton, G. (2017). Dynamic Routing Between Capsules. In *Advances in NIPS*,  
547 pages 3856–3866.
- 548 Santos, T. and Abel, A. (2019). Using Feature Visualisation for Explaining Deep Learning Models In  
549 Visual Speech. In *IEEE ICBDA*, pages 231–235.
- 550 Sharif Razavian, A., Azizpour, H., Sullivan, J., and Carlsson, S. (2014). CNN Features Off-the-shelf: An  
551 Astounding Baseline For Recognition. In *CVPR*, pages 806–813.
- 552 Silver, D., Huang, A., Maddison, C., Guez, A., Sifre, L., Van, G., Schrittwieser, J., Antonoglou, I.,  
553 Panneershelvam, V., Lanctot, M., et al. (2016). Mastering The Game Of Go With Deep Neural  
554 Networks And Tree Search. 529(7587):484.
- 555 Simonyan, K. and Zisserman, A. (2014). Very Deep Convolutional Networks for Large-scale Image  
556 Recognition. *arXiv preprint arXiv:1409.1556*.
- 557 Smilkov, D., Carter, S., Sculley, D., Viégas, F. B., and Wattenberg, M. (2017). Direct Manipulation  
558 Visualization of Deep Networks. In *ICML Workshop on Visualisations for Deep Learning*, volume  
559 abs/1708.03788.
- 560 Springenberg, T., Dosovitskiy, A., Brox, T., and Riedmiller, M. (2014). Striving For Simplicity: The All  
561 Convolutional Net. *arXiv preprint arXiv:1412.6806*.
- 562 Szegedy, C., Liu, W., Jia, Y., Sermanet, P., Reed, S., Anguelov, D., Erhan, D., Vanhoucke, V., and  
563 Rabinovich, A. (2015). Going Deeper With Convolutions. In *CVPR*.
- 564 Tolias, G., Sicre, R., and Jégou, H. (2015). Particular Object Retrieval with Integral Max-Pooling of CNN  
565 Activations. *arXiv preprint arXiv:1511.05879*.
- 566 Xiang, S. and Li, H. (2017). On The Effects of Batch And Weight Normalization In Generative Adversarial  
567 Networks. *arXiv preprint arXiv:1704.03971*.
- 568 Xiao, H., Rasul, K., and Vollgraf, R. (2017). Fashion-mnist: A Novel Image Dataset For Benchmarking  
569 Machine Learning Algorithms. *arXiv preprint arXiv:1708.07747*.
- 570 Yosinski, J., Clune, J., Nguyen, A. M., Fuchs, T., and Lipson, H. (2015). Understanding Neural Networks  
571 through Deep Visualization. In *ICML Deep Learning Workshop*, volume abs/1506.06579.
- 572 Yu, Y., Gong, Z., Zhong, P., and Shan, J. (2017). Unsupervised Representation Learning With Deep  
573 Convolutional Neural Network For Remote Sensing Images. In *ICIG*, pages 97–108.
- 574 Yu, Y., Liu, F., and Mao, S. (2018). Fingerprint Extraction and Classification of Wireless Channels based  
575 on Deep Convolutional Neural Networks. *Neural Processing Letters*, 48(3):1767–1775.
- 576 Yue-Hei Ng, J., Yang, F., and Davis, L. (2015). Exploiting Local Features From Deep Networks For  
577 Image Retrieval. In *Proceedings of IEEE Conference on CVPR*, pages 53–61.
- 578 Zeiler, M. (2012). ADADELTA: An Adaptive Learning Rate Method. *arXiv preprint arXiv:1212.5701*.
- 579 Zeiler, M. and Fergus, R. (2013). Visualizing And Understanding Convolutional Networks. *CoRR*,  
580 abs/1311.2901.
- 581 Zeiler, M. and Fergus, R. (2014). Visualizing and Understanding Convolutional Networks. In *ECCV*,  
582 pages 818–833. Springer.
- 583 Zhang, Y., Zhao, D., Sun, J., Zou, G., and Li, W. (2016). Adaptive Convolutional Neural network and its  
584 Application in Face Recognition. *Neural Processing Letters*, 43(2):389–399.

# Figure 1

Classical CNN Architectures: LeNet and Alexnet

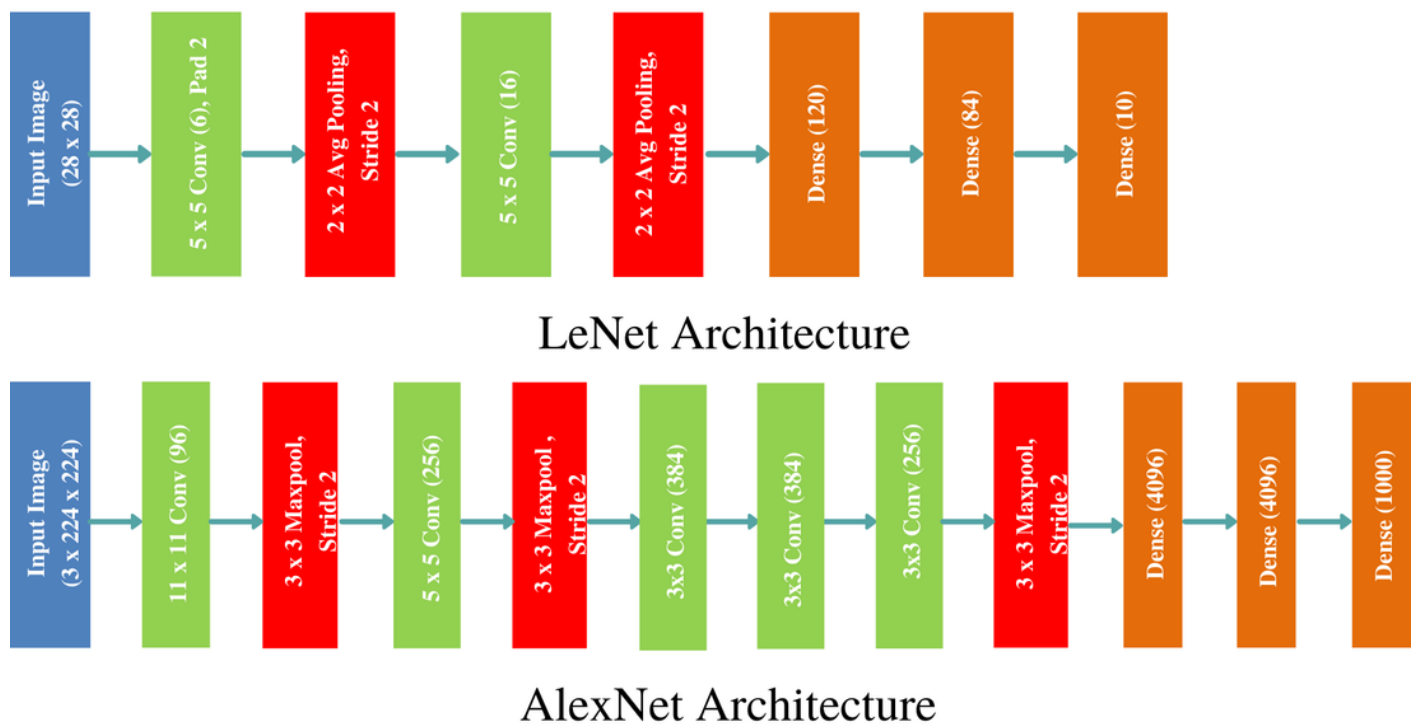


## Figure 2

Graphical abstract of DBAP layer embedded in classical convolutional neural network models for boosting discrimination performance and feature visualisation power.

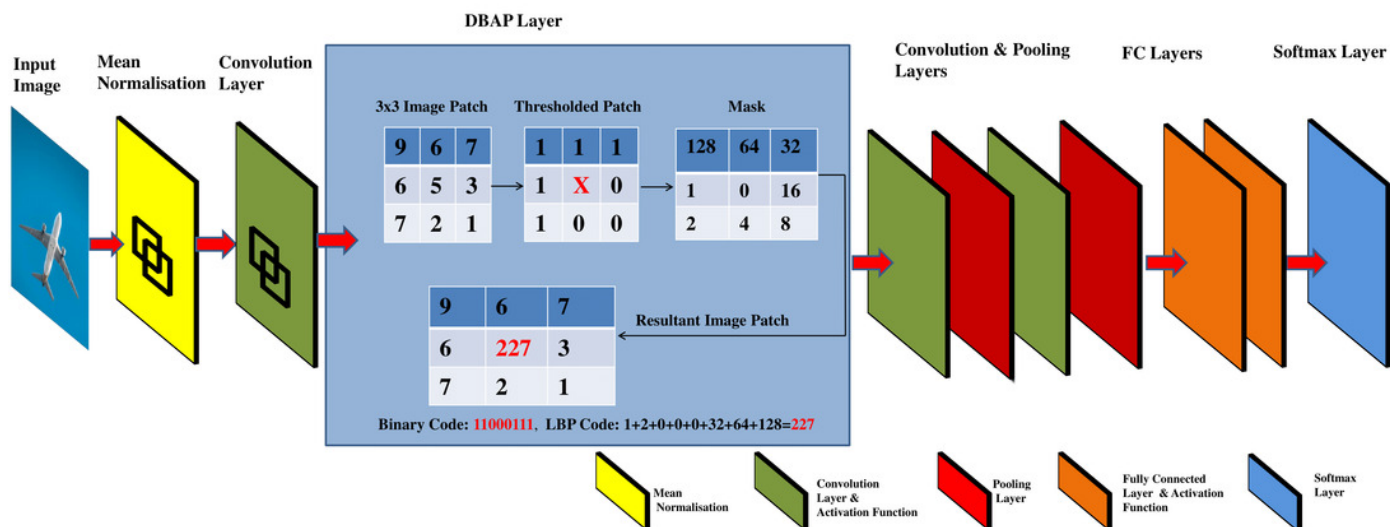
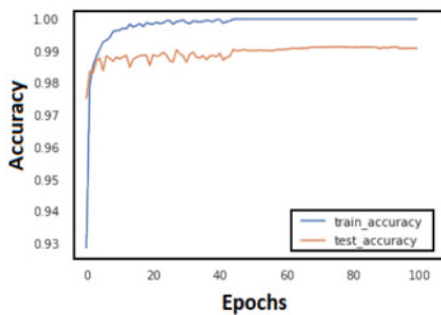
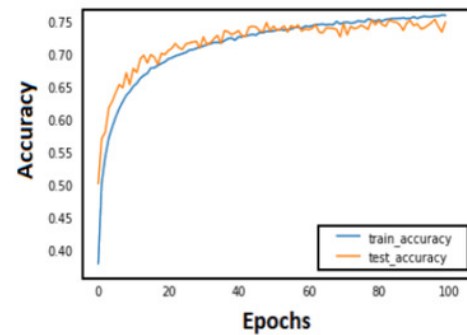


## Figure 3

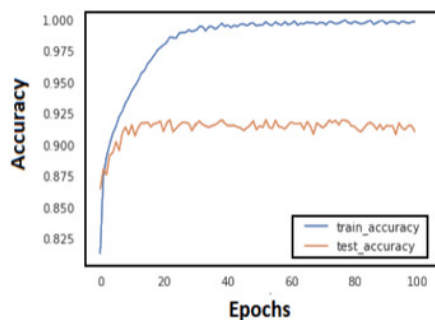
Train and test accuracy curves of LeNet with DBAP layer are demonstrated on state-of-the-art benchmark data sets. The softmax activation function is used to enable LeNet for classification task.



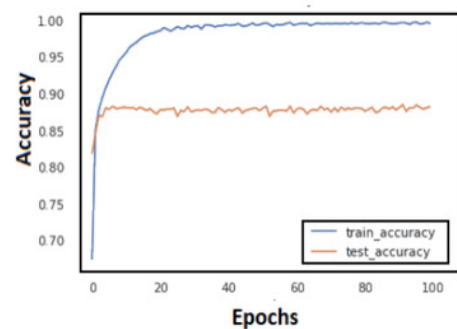
(a) MNIST



(b) CIFAR-10



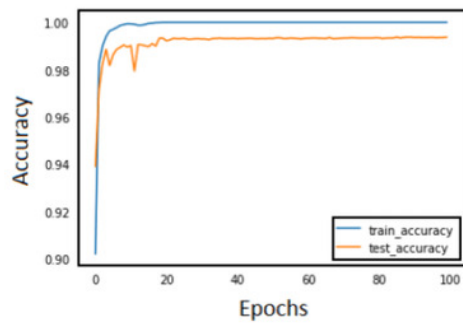
(c) FASHION-MNIST



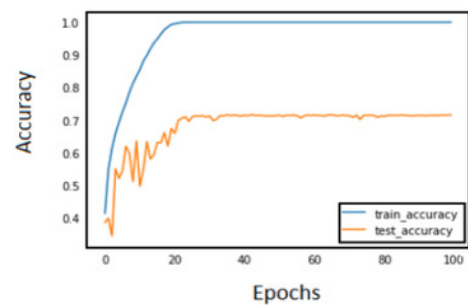
(d) SVHN

## Figure 4

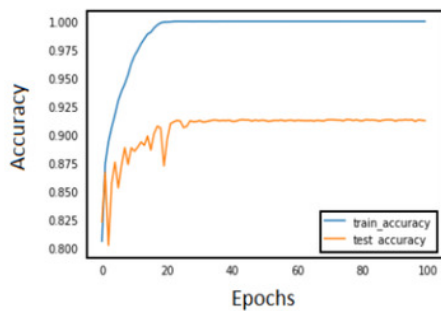
Train and test accuracy curves of AlexNet with DBAP layer are demonstrated on state-of-the-art benchmark data sets. The softmax activation function is used to enable AlexNet for classification task.



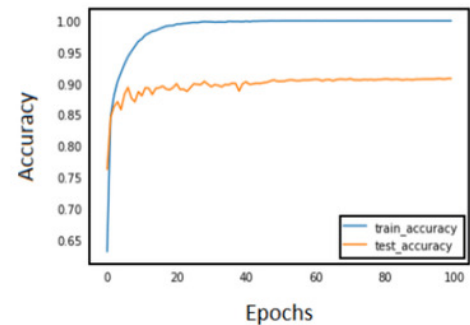
(a) MNIST



(b) CIFAR-10



(c) FASHION-MNIST



(d) SVHN

## Figure 5

Visualising the response of neurons in the MaxPool layer and DBAP layer present in baseline LeNet and LeNet with DBAP layer respectively. With 6 filters/kernels deployed in the first MaxPool layer of LeNet, one can observe that the visualisations of DBAP

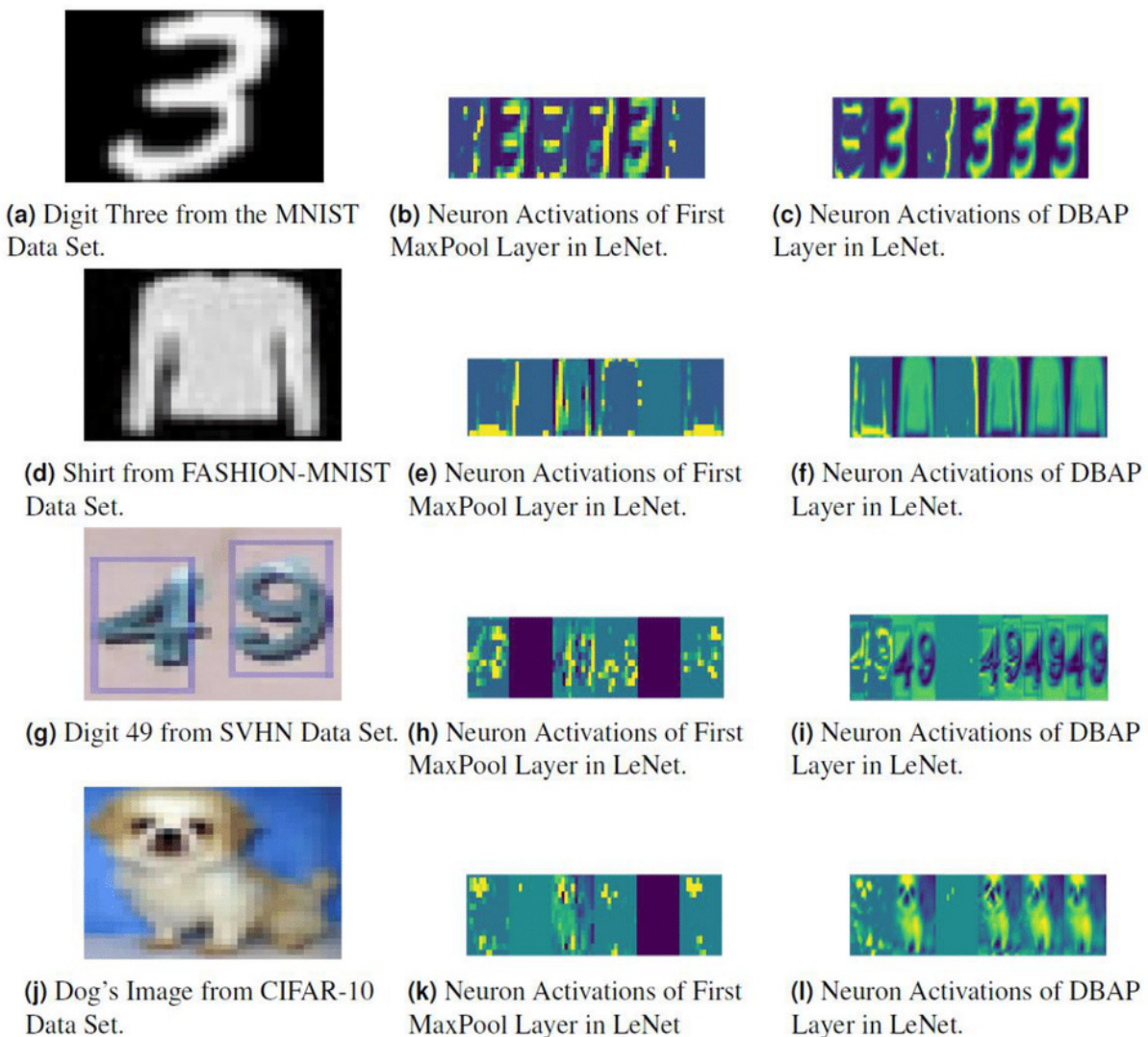


## Figure 6

Visualising the response of neurons in MaxPool layer and DBAP layer with baseline AlexNet and AlexNet with DBAP layer respectively. AlexNet uses 96 filters/kernels of size  $3 \times 3$  in the first MaxPool layer and one can see that DBAP layer retains most

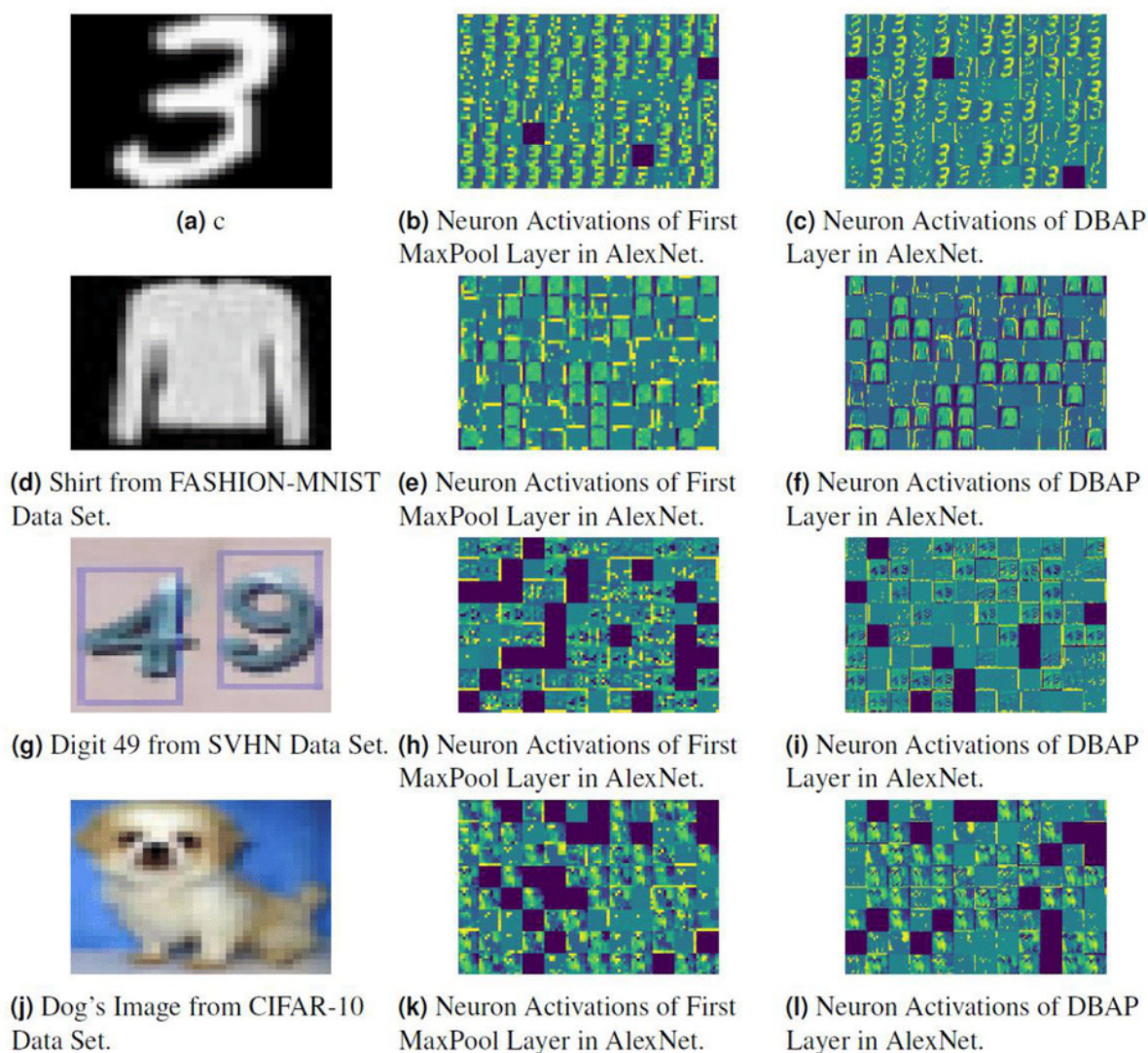
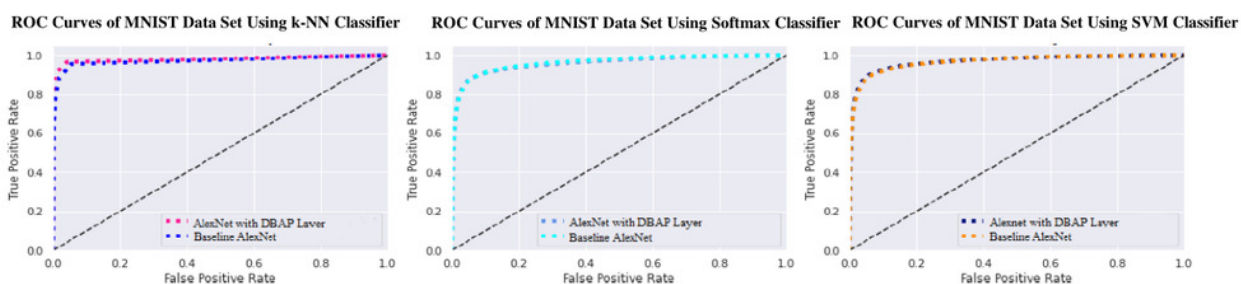


## Figure 7

ROC Curve of k-NN, Softmax and SVM Classifiers on MNIST Data Set.

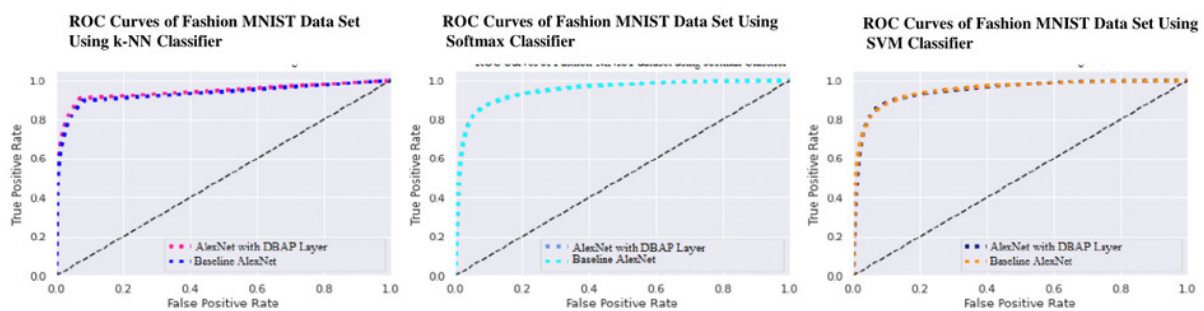


**(a)** AUC with Baseline AlexNet=0.97 & AlexNet with DBAP Layer is 0.98.

**(b)** AUC with Baseline AlexNet & AlexNet with DBAP Layer= 0.96. AlexNet with DBAP Layer= 0.97.

## Figure 8

ROC Curve of k-NN, Softmax and SVM Classifiers on Fashion MNIST Data Set.

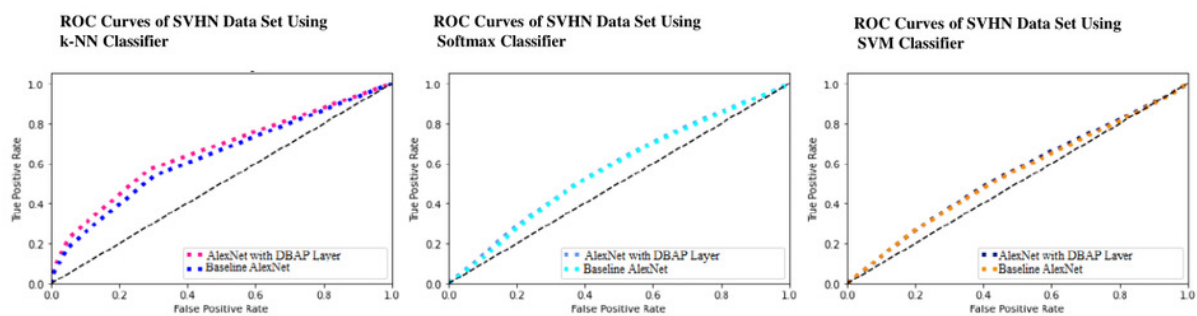


**(a)** AUC with Baseline AlexNet = 0.93 & AlexNet with DBAP Layer = 0.94.

**(b)** AUC with Baseline AlexNet & AlexNet with DBAP Layer = 0.95. AlexNet with DBAP Layer = 0.95.

## Figure 9

ROC Curve of k-NN, Softmax and SVM Classifiers on SVHN Data Set.



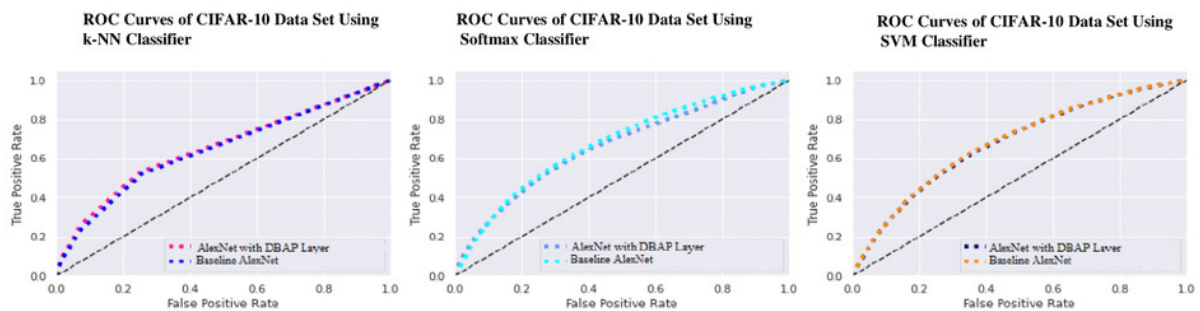
**(a)** AUC with Baseline AlexNet =0.63& AlexNet with DBAP Layer= 0.66.

**(b)** AUC with Baseline AlexNet=0.57& AlexNet with DBAP Layer= 0.58.

**(c)** AUC with Baseline AlexNet=0.54& AlexNet with DBAP Layer= 0.55.

# Figure 10

ROC Curve of k-NN, Softmax and SVM Classifiers on CIFAR-10 Data Set.



**(a)** AUC with Baseline AlexNet=0.64 & AlexNet with DBAP Layer= 0.65.

**(b)** AUC with Baseline AlexNet=0.66 & AlexNet with DBAP Layer= 0.68.

**(c)** AUC with Baseline AlexNet & AlexNet with DBAP Layer= 0.68.